# 3. Technical Components

In this section the specific technical scope of the Recycler upgrade of the Main Injector project is described. For each category of components technical specifications and counts are reviewed.

## 3.1. Magnets (WBS 3.1.1)

Except for a small number of dipole and quadrupole correction magnets, all magnets in the Recycler ring and its associated injection and extraction beamlines are of the permanent variety. In this section the shape, weight, placement, strength, and tolerances of the magnets are described.

### *3.1.1. Recycler Ring Overview*

In the Recycler ring there are 9 unique major magnet types, all of which are permanent magnets. Table 3.1.1 contains name definitions for the magnet types. The two magnet categories which make up the majority of the magnets are gradient dipoles and pure quadrupoles. Figure 3.1.1 and 3.1.2 contains engineering cross-sectional drawings of these two categories.

Table 3.1.1: The definition of names representing magnet types.

| Type | Name | Description |
|---|---|---|
| 1 | RGF | Focusing Gradient Dipole in a Normal Bend Cell |
| 2 | RGD | Defocusing Gradient Dipole in a Normal Bend Cell |
| 3 | RGS | Gradient Dipole in a Dispersion Suppression Cell |
| 4 | RQM | Straight Section Quadrupole |
| 5 | RQS(1-8) | MI-60 Trim Quadrupoles |
| 6 | RQPT(0-4) | MI-60 Phase Trombone Quadrupoles |
| 7 | RLA | Lambertsons at the Ends of Transfer Lines |
| 8 | RMG | Mirror Gradient Dipole near MI-30 Recycler Lambertsons |
| 9 | RVD | Vertical Dipoles for Transfer Lines |

The number of gradient magnets in the ring, along with the design multipole strengths and lengths, are listed for each type of gradient magnet in table 3.1.2. Note that only the normal cell magnets in the region of nominal dispersion contain a sextupole component of the magnetic field in order to combat the natural chromaticity of the uncorrected lattice. It turns out that the present version of the Recycler lattice, version 10, has equal gradient and bend in the focusing and defocusing dispersion suppression gradient magnets. Therefore there are only three pole piece shapes in all of the gradient magnets in the Recycler ring.

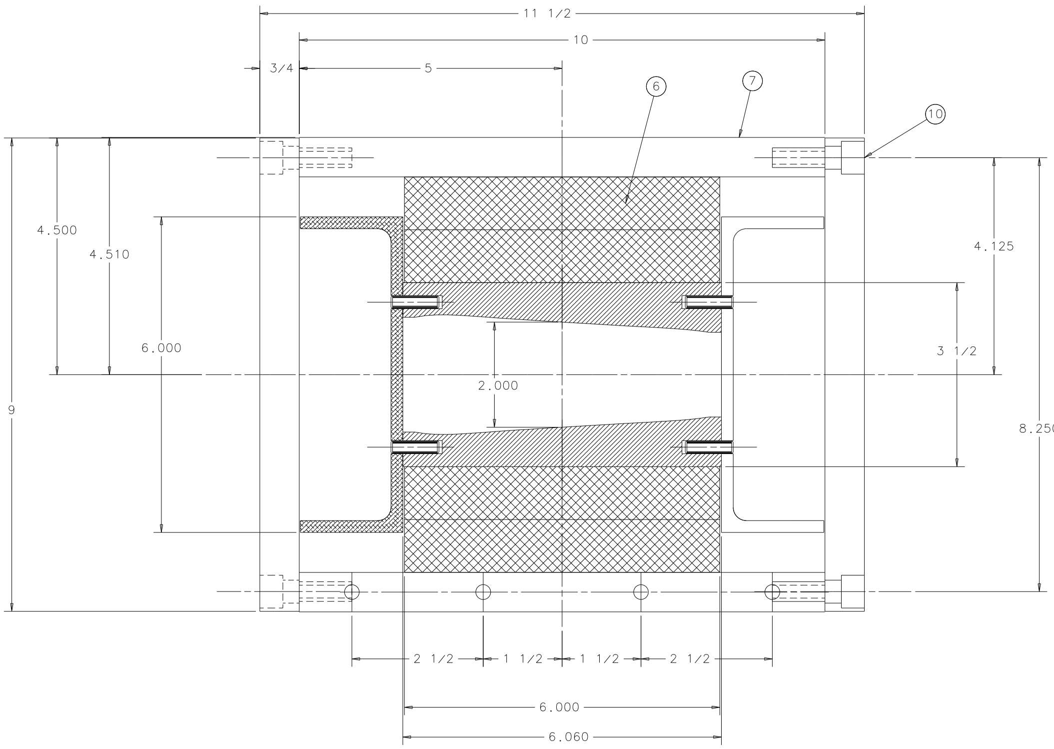


Figure 3.1.1: Gradient magnet profile. These magnets are composed of double bricks on top and bottom.

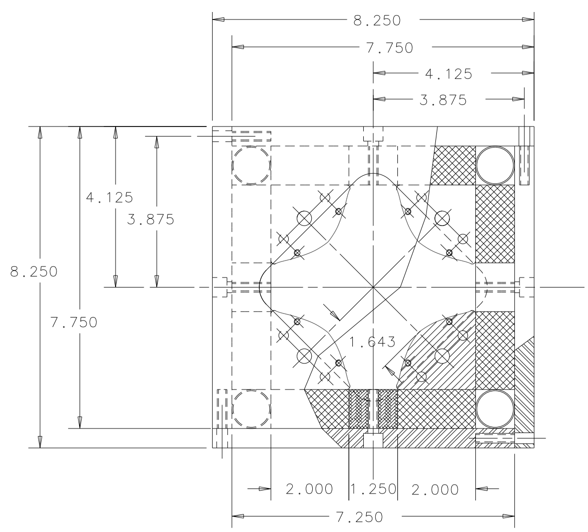


Figure 3.1.2: Quadrupole magnet profile. These magnets are composed of twin cut bricks behind each pole.

The same information for the main quadrupoles in the ring is displayed in table 3.1.3. Note that the focusing and defocusing quadrupoles are identical except for a 90° rotation (or brick polarity reversal during fabrication).

Table 3.1.2: Number, magnetic lengths, and magnetic multipoles of gradient magnets in the Recycler ring. The dispersion suppression focusing and defocusing magnets are now identical. Therefore, there are only three different shape gradient magnet pole pieces in the entire ring.

| Name | Length (m) | Number | $B_o$ (kG) | $B_1$ (kG/m) | $B_2$ (kG/m$^2$) |
|---|---|---|---|---|---|
| RGF | 4.267 | 108 | 1.4494 | 3.515 | 3.566 |
| RGD | 4.267 | 108 | 1.4494 | -3.365 | -5.997 |
| RGS | 2.845 | 128 | 1.4494 | 7.877 | 0 |

Table 3.1.3: Number, lengths, and magnetic multipoles of quadrupole magnets in the Recycler ring. Note that only one pole shape is required in order to produce all of the magnets.

| Name | Length (m) | Number | $B_o$ (kG) | $B_1$ (kG/m) | $B_2$ (kG/m$^2$) |
|---|---|---|---|---|---|
| RQM (F) | 0.5 | 28 | 0 | 26.816 | 0 |
| RQM (D) | 0.5 | 28 | 0 | -25.640 | 0 |

Table 3.1.4: List of the vernier quadrupoles needed on either side of the MI-60 straight section to correct the lattice function distortions caused by the horizontal bypass of the Recycler around the Main Injector RF cavity power tubes.

| Name | Length (m) | Number | $B_o$ (kG) | $B_1$ (kG/m) | $B_2$ (kG/m$^2$) |
|---|---|---|---|---|---|
| RQS1 | 0.5 | 2 | 0 | 6.041 | 0 |
| RQS2 | 0.5 | 2 | 0 | -10.232 | 0 |
| RQS3 | 0.5 | 2 | 0 | -12.926 | 0 |
| RQS4 | 0.5 | 2 | 0 | 19.763 | 0 |
| RQS5 | 0.5 | 2 | 0 | -7.001 | 0 |
| RQS6 | 0.5 | 2 | 0 | -4.235 | 0 |
| RQS7 | 0.5 | 2 | 0 | -9.580 | 0 |
| RQS8 | 0.5 | 2 | 0 | 4.291 | 0 |

At MI-60 the straight section is empty of specialty components except for the four RF cavities. Because of the cost of a distributed quadrupole circuit for betatron tune control of the Recycler, it has been decided to employ the phase trombone method of tune control. By adjusting 5 families of quadrupoles in the MI-60 straight section, the phase advances in the horizontal and vertical planes are independently adjustable while simultaneously maintaining the same Twiss parameter values at the ends. By keeping the end Twiss parameters constant, no lattice mismatches result and the straight section actually appears as a phase trombone. In table 3.1.5 the different settings of the phase trombone quadrupoles are displayed. While holding the maximum beta function in the straight section to under 200 m, a tune range of ±0.5 tune units in either plane can be realized. This maximum beta function value represents an almost doubling of the beam size. A 3" diameter round beam tube will be used in the MI-60 straight section to preserve the admittance of the entire ring.

The initial implementation of these quadrupoles, as well as the two skew quadrupoles required to cancel coupling globally, will be electromagnets - trim quadrupoles reused from the Main Ring and powered by reused Main Ring trim power supplies. A possible later improvement would be to replace the electromagnets with a system to roll adjacent permanent magnet quadrupoles in a counter-phased manner using stepping motors. This would enhance the the high reliability mission of the Recycler. Lattice calculations show that in the rolling scheme three short magnets are required to implement each variable strength quadrupole, but these magnets can also serve as the skew quadrupole correction.

To adjust the beam position and angle through the Lambertson magnets during injection and extraction, and to permit aperture scans, we will install both horizontal and vertical four-bumps at each Lambertson in the Recycler, a total of 24 magnets. These will be reused Main Ring trim dipoles powered by Main Ring trim power supplies. At 8 GeV the Main Ring trims are sufficiently strong, even shimmed to a larger aperture.

Table 3.1.5: Phase trombone quadrupole strengths at MI-60 in a lattice in which the standard phase advance per cell in each transverse plane is maintained.

| Name | Length (m) | Number | $B_0$ (kG) | $B_1$ (kG/m) | $B_2$ (kG/m$^2$) |
|---|---|---|---|---|---|
| RQPT0 | 0.5 | 2 | 0 | -36.676 | 0 |
| RQPT1 | 0.5 | 4 | 0 | 32.033 | 0 |
| RQPT2 | 0.5 | 4 | 0 | -34.601 | 0 |
| RQPT3 | 0.5 | 4 | 0 | 32.679 | 0 |
| RQPT4 | 0.5 | 2 | 0 | -32.827 | 0 |

### *3.1.2. Transfer Line Overview*

There are also a significant number of permanent magnets employed in the three transfer lines associated with the Recycler. The two transfer lines between the Main Injector and the Recycler at MI-30 have the largest number of magnets associated with them, since the transfer occurs over a segment of the tunnel which is bending. Table 3.1.6 contains a summary of the permanent magnets envisioned for both lines. The mirror gradient magnets are required in the Recycler and the beam line at the first (otherwise) normal defocusing gradient dipole downstream (upstream) of the Lambertson. The problem is that the transfer is taking place in a normal arc cell, and the distance between the Lambertson and the first permanent magnet gradient magnet is too small to have both a ring and matching beamline gradient magnet stacked on top of one another. Since the mirror dipoles can be constructed such that there is only 0.75" of flux return for each magnet between the ring and transfer line beam pipes, the minimum separation of 4.5" at the leading edge of the magnets can be accommodated.

Table 3.1.6: Total number of magnets of each type required in both transfer lines at MI-30 between the Main Injector and the Recycler.

| Name | Length (m) | Number | $B_o$ (kG) | $B_1$ (kG/m) | $B_2$ (kG/m$^2$) |
|---|---|---|---|---|---|
| RLA | 4.064 | 4 | 1.5232 | 0 | 0 |
| RVD | 4.267 | 4 | 1.4494 | 0 | 0 |
| RMG | 4.267 | 4 | 1.4494 | -3.365 | -5.997 |
| RQM (F) | 0.5 | 4 | 0 | 26.816 | 0 |
| RQM (D) | 0.5 | 2 | 0 | -25.640 | 0 |
| RGS | 2.845 | 8 | 1.4494 | 7.877 | 0 |

The transfer lines and the abort line all require vertical bends beyond that provided by the Lambertson magnets. The strength, length, and aperture of these magnets match the normal gradients in the ring. Therefore the plan is to copy the design, substituting a new pole shape to produce a dipole field.

In the proton abort line three 20 mrad permanent magnet dipoles and two quadrupoles are necessary. In addition, a mirror dipole or permanent magnet Lambertson is also needed. These counts are summarized in table 3.1.7.

Table 3.1.7: Total number of magnets of each type required in the Recycler abort line.

| Name | Length (m) | Number | $B_o$ (kG) | $B_1$ (kG/m) | $B_2$ (kG/m$^2$) |
|---|---|---|---|---|---|
| RQM | 0.5 | 4 | 0 | 26.816 | 0 |
| RLA | 4.064 | 2 | 1.5232 | 0 | 0 |
| RVD | 4.267 | 3 | 1.4494 | 0 | 0 |

### *3.1.3 Permanent Magnet Design Features*

The basic design of the permanent magnet dipole is shown in figure 3.1.3. It is a 1.5 kG gradient (combined-function) dipole with a 2 in. gap at the center, a 5.5 in. horizontal aperture and a 3.5 in. horizontal good-field aperture. Overall dimensions are 9.5 in. high by 11.5 in. wide by approximately 13 ft. long. The weight is typically 2000 lb. The magnets are straight and the sagitta of the beam inside a magnet is typically 1 cm. The beam pipe dimensions under vacuum are approximately 1.75 in. vertically and 3.75 in. horizontally. The precise parameter values for each of the individual gradient magnet types appear in table 3.1.8.

The design is a so-called “hybrid” permanent magnet in which the field is driven by permanent magnet material and the field shape is determined mainly by steel pole pieces. The field quality, which is shown in figure 3.1.4, is designed to give a vertical magnetic field error of less than $1\times10^{-4}$ across the designated good field region. The permanent magnet bricks drive flux into (from) the pole tips from the top (bottom) (see figure 3.1.5). The entire assembly is enclosed in a flux return shell 0.75” thick. Solid "bar stock" components are used throughout rather than laminations. The pole tip steel is 1008 low carbon steel and the flux return is construction grade (A36) steel. The design field harmonics which correspond to the design shape shown in figure 3.1.4 are listed in table 3.1.9.

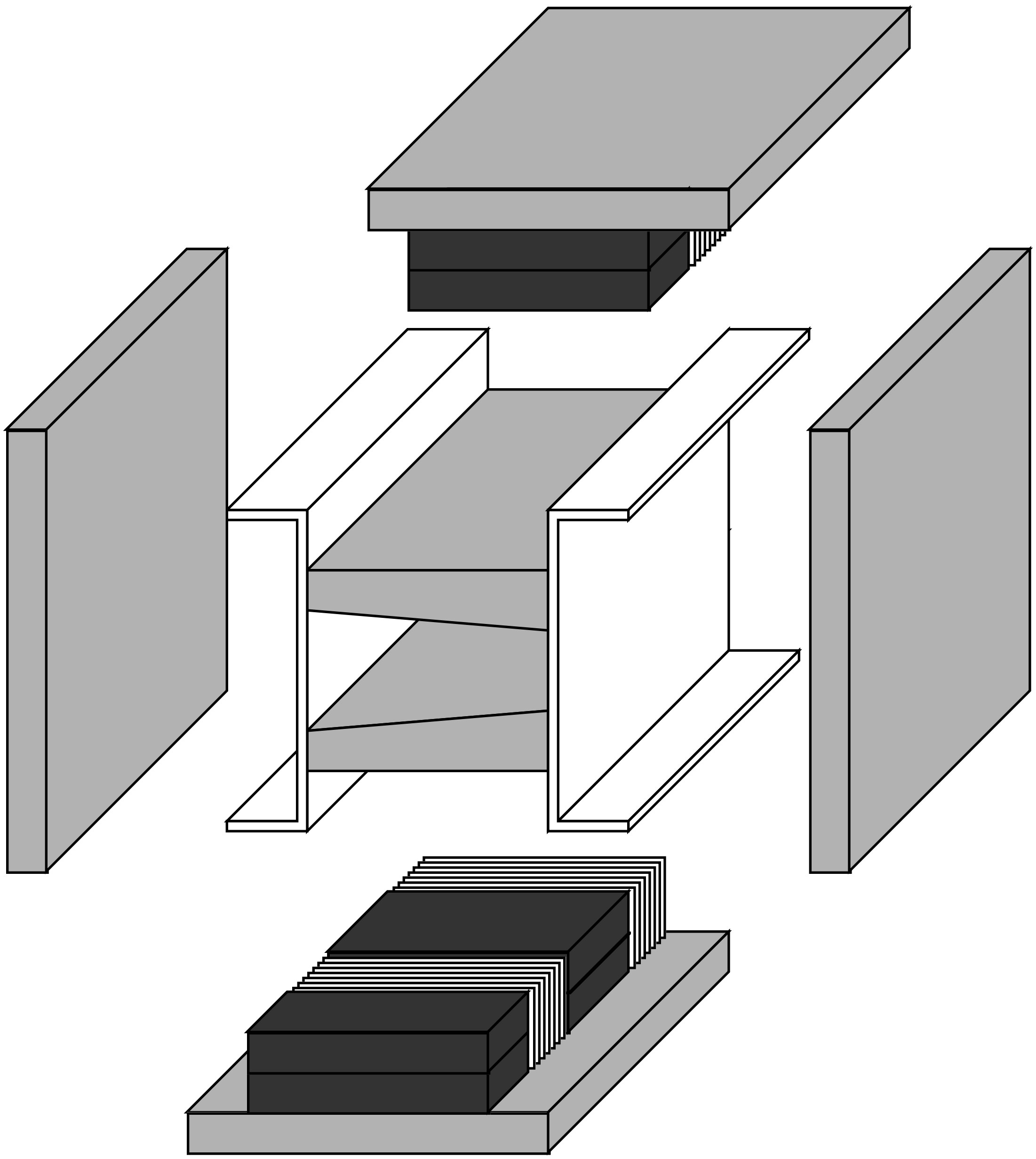

Figure 3.1.3: Permanent magnet gradient dipole components shown in an exploded view. For every 4" wide brick there is an 0.5" interval of temperaature compensator material composed of 10 strips.

Table 3.1.8: Design and physical parameters of Recycler focusing (RGF), defocusing (RGD), and dispersion suppresser (RGS) gradient magnets.

| Parameter | RGF | RGD | RGS |
|---|---|---|---|
| Magnet Width (in.) | 11.5 | 11.5 | 11.5 |
| Magnet Height (in.) | 9.0 | 9.0 | 9.0 |
| Physical Length (in.) | 175.0 | 175.0 | 119.0 |
| Total Weight (lb.) | 2691 | 2691 | 1800 |
| Magnetic Length (in.) | 168.0 | 168.0 | 112.0 |
| Bend Angle (mrad) | 21 | 21 | 14 |
| Beam Sagitta (mm) | 10 | 10 | 5 |
| Flux Return Weight (lb.) | 1496 | 1496 | 1017 |
| Pole Tip Weight (lb.) | 302 | 302 | 202 |
| Ferrite Brick Weight (lb.) | 710 | 710 | 461 |
| Compensator Weight (lb.) | 133 | 133 | 86 |
| Aluminum Weight (lb.) | 50 | 50 | 34 |

Table 3.1.9: Calculated magnetic field harmonics for the Recycler arc cell focusing gradient magnet pole shape design.

| N | Normal | Skew | N | Normal | Skew |
|---|---|---|---|---|---|
| 1 | 10000 | -0.07 | 7 | 0.02 | -0.02 |
| 2 | 610.03 | 0 | 8 | 0 | 0.01 |
| 3 | 15.21 | -0.06 | 9 | 0.04 | 0.01 |
| 4 | -0.11 | 0 | 10 | 0.01 | -0.02 |
| 5 | -0.1 | -0.02 | 11 | -0.07 | 0.01 |
| 6 | 0.01 | -0.01 | | | |

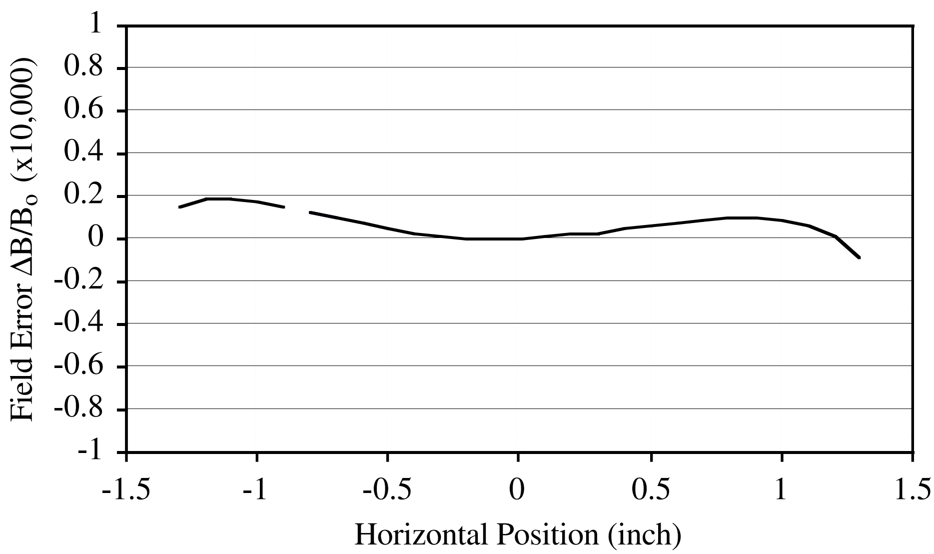


Figure 3.1.4: Design magnetic field imperfection across the horizontal aperture of a Recycler gradient magnet. Generated by Poisson, the ripple in the field is due to the finite extent of the poles and the trapezoidal approximation of the pole shape.

As shown in figure 3.1.6, the end fields of the magnets are terminated by flux clamp/end plate assemblies which are magnetically connected to the flux return shell. These plates prevent the stray flux from leaking out and saturating the mu-metal/soft iron shielding of the beam pipe between magnets. The end plates are removable to allow access to the ends of the pole tips for field quality shimming operations.

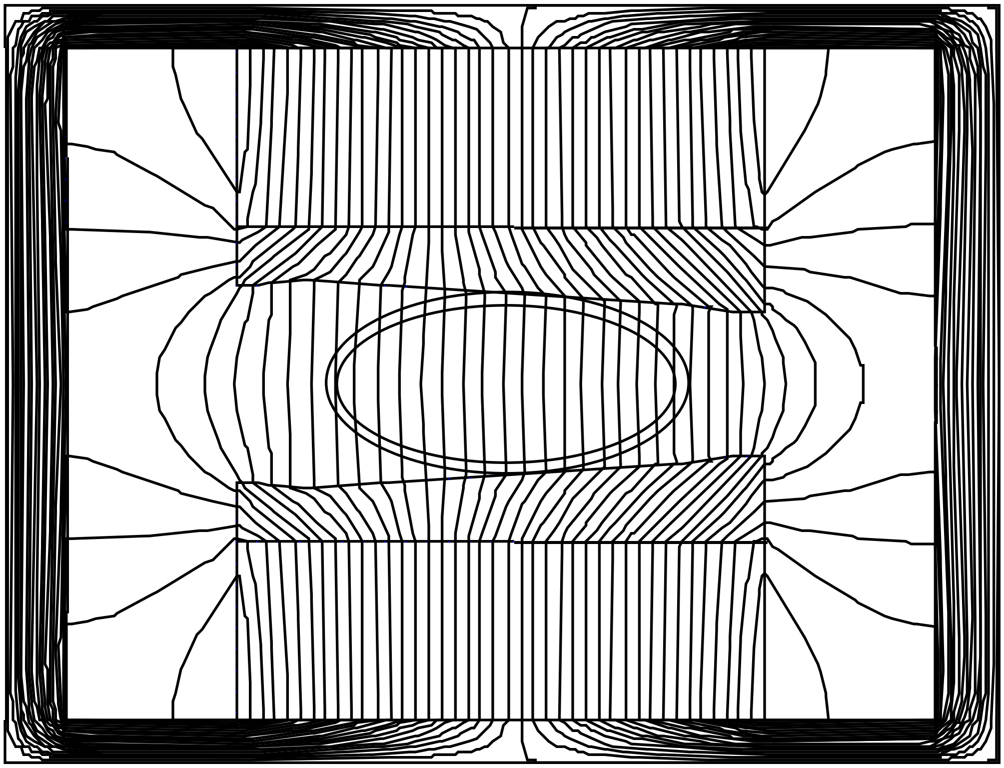

Figure 3.1.5: POISSON field map of a Recycler gradient dipole.

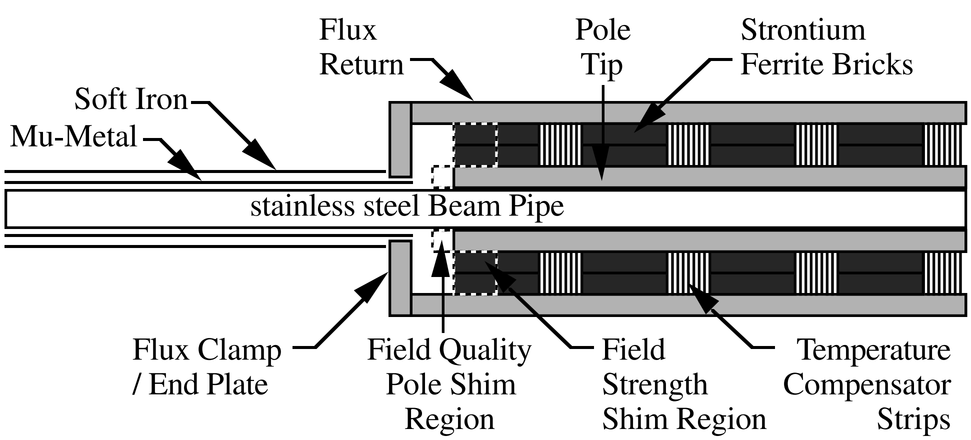


Figure 3.1.6: Side view of magnet, showing transition from magnetic shielding of naked beam pipe to magnet flux return. Also indicated are the regions at the ends of the pole tips devoted to shimming the field shape, and the ends of the ferrite bricks which are used to trim the strength of the magnet by adjusting the total amount of magnetic material.

### *3.1.4. Permanent Magnet Material*

We have chosen Type 8 Strontium Ferrite (Type 8 Strontium Ferrite data sheets & specifications from Arnold, Crucible, and Hitachi) as the permanent magnet material because of its low cost and high stability over time, temperature, and radiation. Strontium ferrite is the material of choice in automotive applications and is available at low cost in standard grades and sizes from multiple vendors. It has documented stability in applications such as NMR magnets and is commonly used in ion pumps in accelerator applications. Materials from the three major U.S. vendors were evaluated and performed well in the R&D program.

### *3.1.5. Magnetization and Strength Trimming*

Ferrite bricks are shipped unmagnetized from the foundry and are magnetized immediately prior to assembly using a 2 Tesla dipole. The bricks are individually measured and assembled into "kits" each containing a specified total magnetic strength of brick. The magnet design is such that a magnet fully loaded with bricks of nominal strength is 3~5% stronger than required. Dummy bricks, fractional bricks and spacers are used to control the total strength of the "kits" to correct for brick-to-brick and lot-to-lot variations. A final strength trim is accomplished by adjusting the amount of ferrite at the ends of the magnet.

### *3.1.6. Temperature Compensation*

The intrinsic temperature coefficient of the Ferrite material (-0.2%/°C) is canceled [Dallas 1995 PAC papers on permanent magnets by Bertsche & Ostiguy, Foster & Jackson] by interspersing a "compensator alloy" (Carpenter Technologies Compensator 30 type 4 data sheets from Telcon data sheet, Eagle Alloys, Sumitomo Heavy metals) between the ferrite bricks above and below the pole tips. The compensator is an iron-nickel alloy with a low Curie temperature and therefore a permeability which depends strongly on temperature. This shunts away flux in a temperature dependent manner which can be arranged to null out the temperature dependence of the ferrite. We find that the degree of temperature compensation is linearly related to the amount of compensator material in the magnet. Thus the degree of compensation can be "fine tuned" to the required accuracy by adjusting the amount of compensator at the ends of the magnet in a manner similar to the strength trimming with the ferrite. For example, a 20-fold reduction of the temperature coefficient (from 0.2%/°C to 0.01%/°C) requires that the amount of compensator in the magnet be adjusted correctly to 1 part in 20. This poses no difficulties for production.

The range and accuracy of the required temperature compensation is determined by the expected variation in tunnel temperature. Data from the Main Ring tunnel during a typical period of operations can act as a guide to predict Main Injector tunnel temperatures. Figure 3.1.7 contains data from a Main Ring sector which had the maximum temperature variation during the time plotted. Note that a ±1°C temperature variation is a pessimistic estimate.

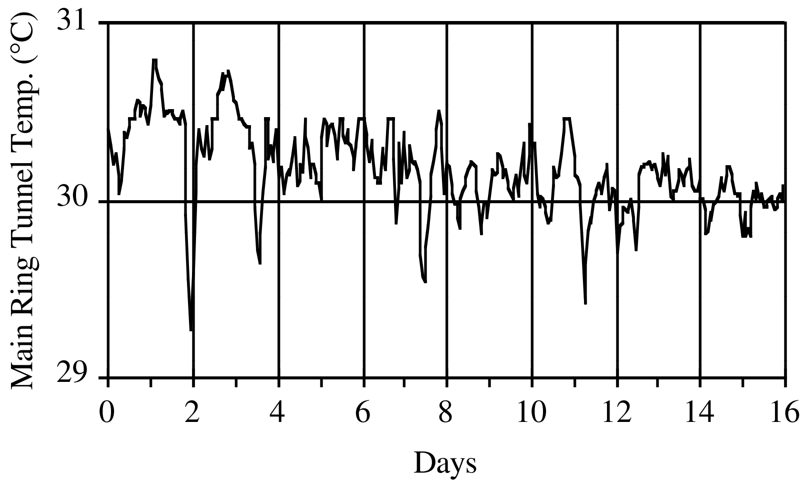


Figure 3.1.7: Measured Main Ring tunnel temperature during a typical period of operations. Note that on the second day the Main Ring was turned off for a few hour access.

The ultimate limit to the temperature range of the compensation technique is set by the nonlinearities of the opposing temperature coefficients. The ferrite material appears to be highly linear over the relevant temperature range. However, the compensator material tends to become weaker as it approaches its effective Curie temperature of approximately 55°C. Figure 3.1.8 indicates the degree of compensation achieved on a test magnet using ferrite and compensator materials from the 8 GeV line production (low bidder) vendors. Note that the maximum deviation is $\pm 1 \times 10^{-4}$ over the range 31± 7 °C.

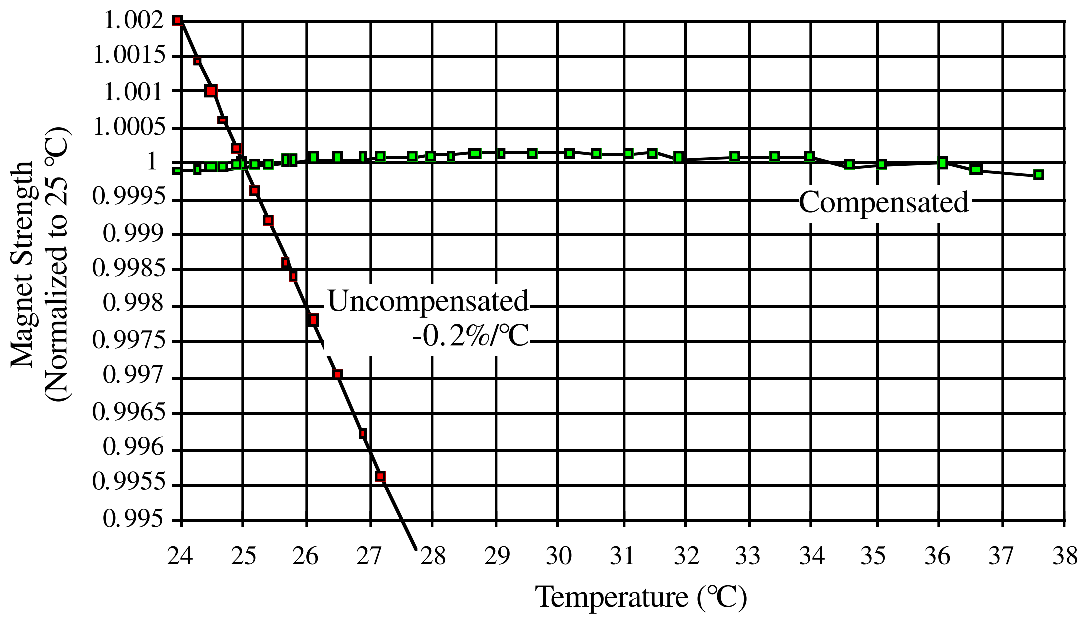


Figure 3.1.8: Field strength vs. temperature for a stability test magnet using pre-production samples from the selected vendors for compensator alloy and ferrite.

### *3.1.7. Magnet Assembly*

The assembly sequence is as follows (see figure 3.1.3). The pole pieces are pinned and bolted to the aluminum U channel side members hold them in place to make a box structure. The bricks are placed on the back of the pole pieces, interleaved with the strips of compensator. The magnetic forces hold them in place. The top and bottom flux return plates are lowered onto the assembly using meachanical fixturing to control the operation in the presence of strong magnetic forces. The side flux returns are then moved to their places using the fixturing and bolted to the top and bottom plates. The steel end plates are installed and bolted to the flux return.

After the initial assembly each magnet's field strength and shape will be measured at the assembly facility. On the basis of this shape measurement, the steel shim pieces described below will be machined to trim the field shape as needed. In parallel the magnet will be placed in a large freezer and cooled to 0 degrees C to stabilize it against further temperature excursions (see section 3.1.9 Stabiliy Issues) during installation. On removing the magnet from the freezer the temperature and strength will be measured immediately. Assuming that the magnet is correctly compensated, the strength trimming can be determined from this measurement. After the magnet warms to room temperature, the strength will be remeasured to verify that it is correctly compensated, then the end shims will be installed and the appropriate bricks added or removed to trim the strength. A final measurement will confirm that the correction was successful and document the final configuration.

### *3.1.8. Field Quality*

The field quality of the Recycler magnets must be adequate for a storage ring, i.e. roughly $\Delta B/B = \pm 0.01\%$ over a good-field aperture chosen to be 1.75 in. horizontal by 3.5 in. vertical, or $\pm 0.02\%$ over $\pm 25$ mm in the performance simulations. The basic manufacturing strategy is to maintain construction tolerances of a few times 0.001 in. for the iron pole tips of the magnets, which is sufficient to achieve roughly 0.1% field defect over the aperture. The field shape is then trimmed to an accuracy of 0.01% using additional metal pieces on the ends of the magnet pole tips. This procedure is considerably simplified since only the integrated field is of interest, and the shims only have to work at a single level of excitation (no saturation effects).

### *3.1.9. Stability Issues*

In order to address the issue of long-term stability of strontium ferrite, 10 test dipoles "stability test magnets" were built and subjected to a variety of environmental conditions which could possibly have an impact on the magnetic stability. The effects studied included varying the ferrite and compensator suppliers (most of the stability magnets were built with Hitachi bricks and Carpenter type-4 compensator), heating and cooling effects, radiation, partial demagnetization of the bricks, and simple aging.

One effect which has so far been demonstrated to have an immediate and irreversible effect on the magnet strength is cooling below 0°C. A magnet was cooled from room temperature (20°C) to 10°C, and no decrease in strength was seen when warmed back up to room temperature. However, on freezing to 0°C, the magnet lost 0.05% of its original strength on warm-up. It was then cooled to -20 C, and it lost 0.1% of its original strength. This magnetization loss appears to be a one-time effect, provided one does not cool the magnet below the previous coldest temperature it has experienced. Thus, the magnet was cooled a second time to -20 C, and did not suffer any additional degradation in strength. This effect has been observed on two different magnets.

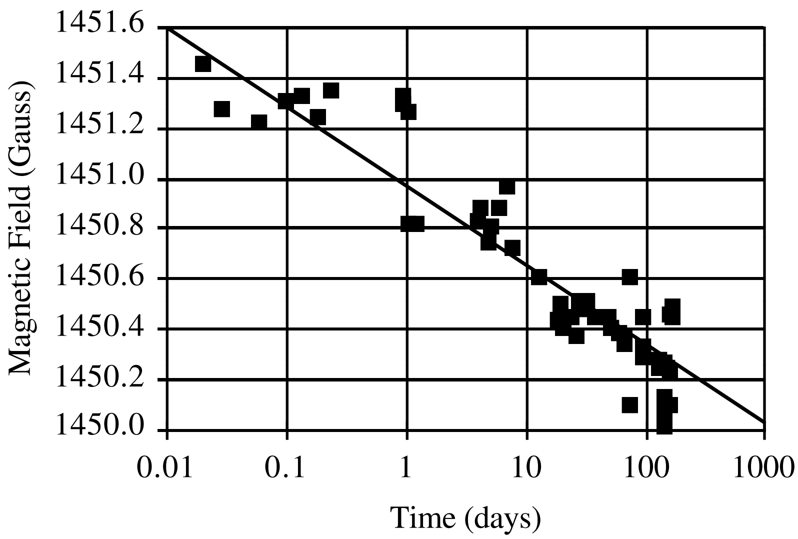


Figure 3.1.9: Field strength vs. time of a stability test magnet. Over 4 decades the data follows an expected log-time dependence. The line represents a log-time decay rate of $2.2 \times 10^{-4}$/decade.

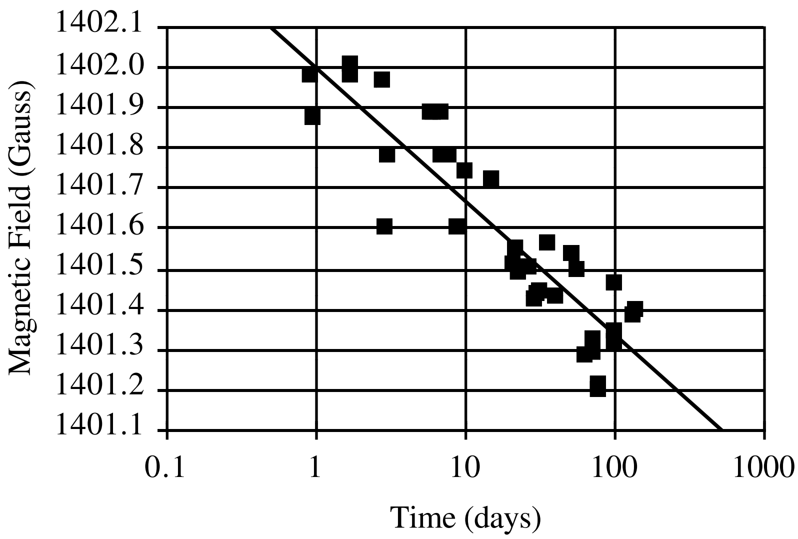


Figure 3.1.10: Field strength vs. time of a stability test magnet. This magnet was composed of bricks which were demagnetized by 5% before assembly. The line represents a log-time decay rate of $2.4 \times 10^{-4}$/decade.

Some magnets were monitored for aging by measuring their strength (at the midpoint of the aperture, using an NMR probe) as a function of time since production. The data, shown for two magnets in figures 3.1.9 and 3.1.10, is consistent with an expected log-time aging [Kronenberg & Bohlmann, J. Appl. Phys. **31**, 82S (1960); Street & Wooley, Proc. Phys. Soc. **A62**, 562 (1949)], and the present upper limit on aging derived from this data ($2.5 \times 10^{-4}$/decade) corresponds to less than 0.05% of field change over a 20-year life span for the magnets. Aging at this level can be easily accommodated by changing the energy of the Booster, Main Injector, Debuncher, and Accumulator rings to match the central energy of the Recycler.

One magnet was irradiated by a source putting out approximately 0.8 Mrad/hour for 268 hours. Taking into account down time, the net average flux to the magnet was about 0.3 Mrad/hour for about 100 Mrads. The observed change in magnet field is approximately 0.5 Gauss out of 1465 Gauss, or $\sim 3 \times 10^{-4}$ which is within the range of allowed variation. No change was seen in a series of low level initial doses. In addition, mechanical disturbance such as dropping the magnet had no measurable effect above 0.3 Gauss.

One concern voiced in some project reviews was the potential for strength demagnetization of the Recycler permanent magnets due to the A.C. component of the stray fields in the tunnel from Main Injector components. A 1 m long prototype of an arc cell focusing gradient magnet was exposed to 100 magnetic field ramps generated by a Helmholtz coil. With an estimated field in excess of 10 Gauss, no observable field loss (to an accuracy of $1 \times 10^{-5}$) was observed.

Another review concern was changing of the field magnitude or shape from the 150°C in-situ bake of the vacuum system. ANSYS calculations of the bake procedure predict that the permanent magnet bricks never exceed 40°C due to thermal insulation around the beam pipe and heat transport through the aluminum and steel components out to the air. In order to verify theoretical predictions that this temperature is not harmful to the magnetic field of gradient magnets, the 1 m long prototype magnet was heated to a uniform temperature of 60°C. No field strength or quality changes were observed.

### *3.1.10. Magnet Measurement Requirements*

A rotating coil probe has been built for measuring all of the dipole and gradient magnets for the 8 GeV and Recycler projects. This probe is a Morgan-style probe, having windings sensitive to dipole through 14-pole. It is 16 feet in length, which allows measurements of integrated strength of all the anticipated magnets. Morgan probes have the advantage of cleanly separating dipole, quadrupole, and higher-order harmonics, an essential feature for measuring gradient magnets. The probe has been tested on the two pre-production magnets, and has demonstrated the ability to meet the specified requirements of measuring the integrated strength to better than $2 \times 10^{-4}$ and the harmonics to about 0.2 units (0.2 parts in 10,000 at 1 in.). An additional probe with a tangential winding geometry is being considered to improve the sensitivity to higher magnetic field multipoles.

A redundant measurement system will use a single stretched wire to scan the horizontal aperture. This device will provide a second measurement of the strength, but will also map the field shape in a region inaccessible to the Morgan coil (beyond

$|x|>0.8$ in.). This stretched wire system has been in use in measuring Main Injector quadrupoles.

A Hall probe measurement system to measure the central field as a function of the longitudinal position will be necessary. A similar system is used in the Main Injector dipoles. The field strength profile of the magnet as a function of distance inside the magnet must be generated with sufficient resolution to determine the bend center to approximately 0.5".

### *3.1.11. Field Shape Tuning*

Using the two full length gradient magnets already produced for the 8 GeV line project, studies have been performed attempting to identify an algorithm for tuning the field harmonics to a level required by lattice and beam stability criterion. Because these magnets do not change in field, end packs shaped to eliminate unwanted field harmonic amplitudes are relatively simple to employ. Tests show that field deviations across the aperture as large a 0.1% can be corrected.

We now have experience with constructing identical models of full length Recycler gradient magnets. Figure 3.1.11 shows the multipole difference between two magnets built identically. Repeated measurements were performed on each magnet, and the difference RMS is shown to give one a feeling of the expected error bars on these measurements. The dominant error is in the normal gradient, which is easily tuned with end shims discussed in the next paragraph. The skew multipole differences are generated by a pole potential imbalance caused by unequal brick strengths behind the top and bottom poles (before equalization was carried out). In experiments with equalization the transfer function between brick strength and skew multipole strength has been measured. The results of these measurements scaled to the observed difference in these two magnets are also displayed. The dominant source of skew moment is this easily correctable pole potential imbalance.

As shown in figure 3.1.12, the shimming is presently accomplished by adding extra sections of gradient poles which are shaped longitudinally in order to generate the required multipole correction. These shapes are generated by measuring the field deviation in each magnet, using the measurement program to generate an input file for a computer controlled wire EDM machine, cutting a piece of normal pole piece, and then mounting the extra pole pieces (one top and one bottom) on one side of the magnet. The lower the multipole moment, the bigger a multipole correction can be made for a given average shim thickness. As can be seen in figure 3.1.11, the higher the multipole moment the smaller the multipole error which can be generated with expected fabrication imperfections.

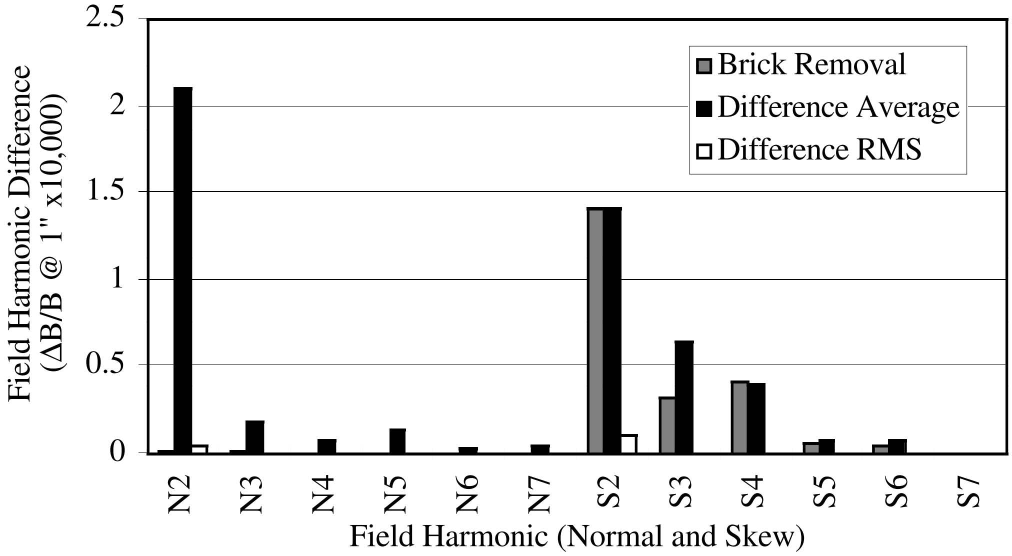


Figure 3.1.11: Difference in magnet field quality due to difference in magnet fabrication measured on two identical full length Recycler prototype gradient magnets.

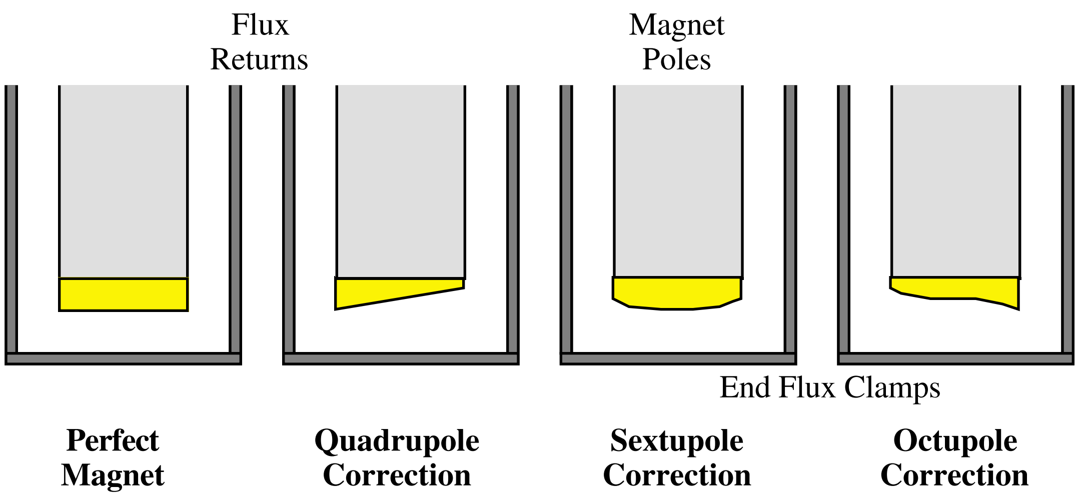


Figure 3.1.12: Sketch of the scheme used to correct any measured field shape errors. Using these prototype shapes and linear superposition, a very good correction algorithm has been generated and measured.

### *3.1.12. Recycler Magnet Key Performance Specifications*

The table below contains the basic key specifications for the Recycler permanent magnets. These are discussed, justified, and quantified at exhaustive length in MI-Note #150. Many of the values listed in this table, such as the design lifetime, are rather arbitrary and are intended to guide engineers and technicians toward an appropriate level of care and ruggedness.

Table 3.1.10: Miscellaneous magnet performance specifications. Many of the specifications are quite far from anticipated parameter values and do not present concerns.

| | |
|---|---|
| Design Lifetime | 30 years |
| Operating Temperature | 20°C (68°F) to 35°C (95°F) |
| Storage Temperature | 5°C (41°F) to 50°C (120°F). |
| Humidity | 0%-100% |
| Corrosion Resistance | All parts resistant, plated, or painted. |
| Bakeout Compatibility | Beam Pipe @ 150°C, Magnet @50°C |
| Temperature Stability of Field Strength | ±0.05% full spread over 10-35°C |
| Temperature Stability of Field Shape | < ±1 unit in any multipole for ±10°C |
| Time Stability | $\Delta B/B$ < 0.05%/yr. |
| Radiation Resistance | $\Delta B/B$ < 1% for 1E9 Rads |
| Shock & Vibration | $\Delta B/B$ < 0.1% from normal handling |
| Radiation Activation | Comparable to steel/copper magnets |
| Good-Field Aperture | ±1.25" at $\lvert \delta By/B_0 \rvert$<1E-4 |
| Dipole Vertical Aperture | 2.0" between the pole tips (at X=0) |
| Quadrupole Pole Tip Radius | 1.643" (XY = 1.350 in$^2$, same as MI) |
| Magnet Sagitta | Zero (straight magnets) |
| Beam Sagitta Inside Dipole | ~1cm |
| Field Uniformity in Z | ±5% (random) or better |
| Bend Center uncertainty | ±1cm in Z (measured and surveyed) |
| Field Strength Modification | possible in range [+3%,-5%]. |
| Field Shape Modification | +/- 10 units (modify end shims) |
| Magnetic Field in Flux Return | <1 Tesla |
| Magnetic Shielding of Beam Pipe | 2-layer (μ-metal + iron foil) |
| Termination of End Fields | via Flux Clamp / End Plate of Magnets |
| End Fields | < 5 Gauss 2.5 cm past end of magnet |
| Beam Pipe Fixturing | allows ±1cm horiz. range of motion |
| Survey Fiducials | 8 "nests" at corners of magnet |
| Mechanical Rigidity (sag) | < 0.020" for 25% , 75% support points |

### *3.1.13. Permanent Magnet Quadrupoles*

One type of permanent quadrupole is required for the Recycler. The standard design has the same 1.643" pole tip radius as the Main Ring/Main Injector quadrupoles. All Recycler quadrupoles are 0.5 m long. Different strengths are implemented with different brick concentrations and flux shorting shims.

The quadrupoles have a hybrid design analogous to the gradient dipole. The field shaping is provided by machined steel pole tips and the field is driven by strontium ferrite bricks. The version which is currently under fabrication for the 8 GeV line and Recycler R&D is shown in figure 3.1.13. Temperature compensation of the ferrite is provided by interspersing strips of compensator alloy between the bricks along the length of the magnets. The overall strength of the magnet is trimmed by adjusting the amount of permanent magnet material behind each pole tip, and the field shape is trimmed by adding steel shims to the ends of the pole tips. A steel flux return shell surrounds the magnet, and "flux clamp" end plates are used to terminate the field at the ends of the magnet.

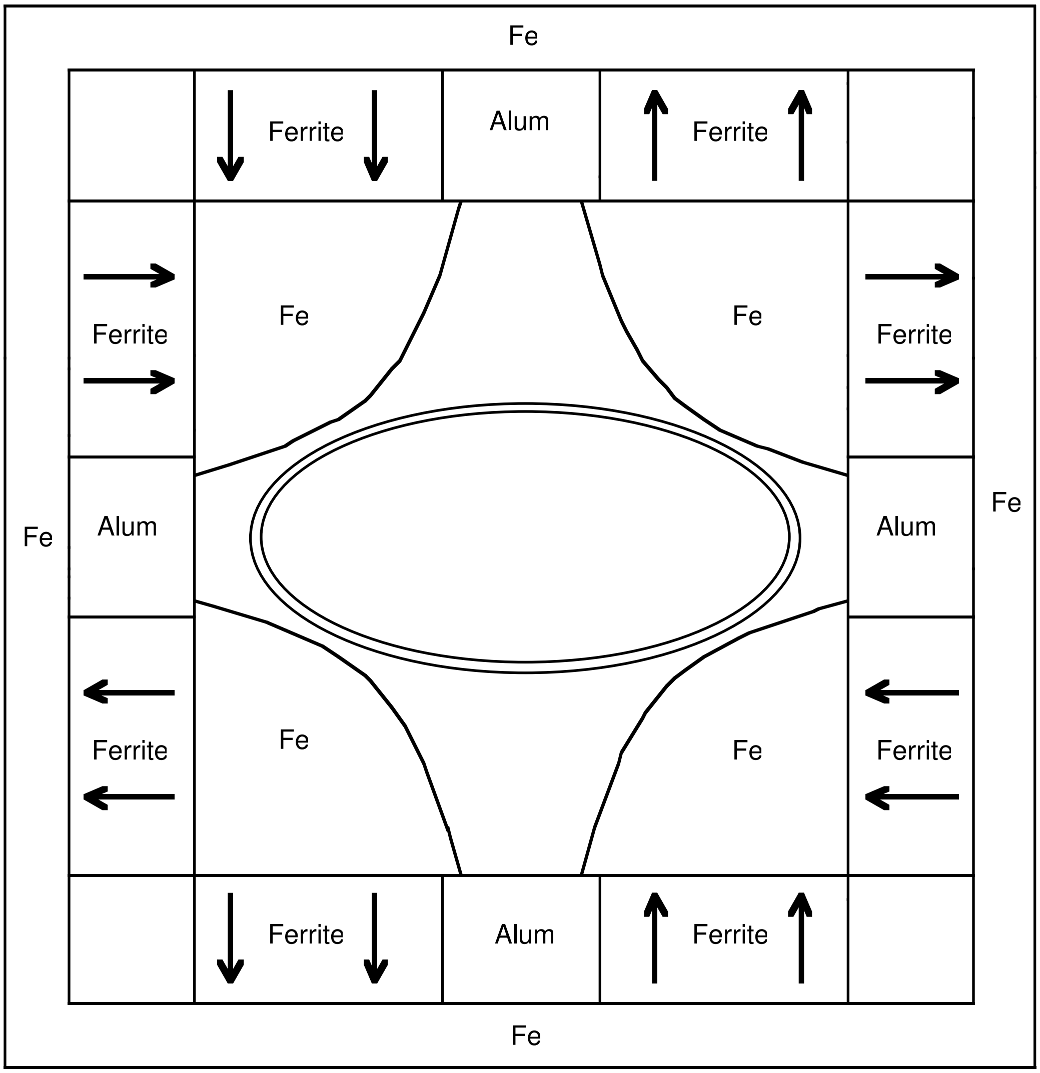


Figure 3.1.13: Cross-section of a rectangular quadrupole magnet.

## *3.1.14. Permanent Magnet Lambertsons*

Transfer lines to and from the Recycler and 8 GeV line require a total of six Lambertson magnets. A standard design (2 kG, 3m long) has been adopted which provides a 21 mrad bend for the 8.9 GeV/c extracted or injected beam. In the typical application the circulating beam is in the field-free region and is kicked horizontally outwards into the bend region where it is deflected upwards or downwards.

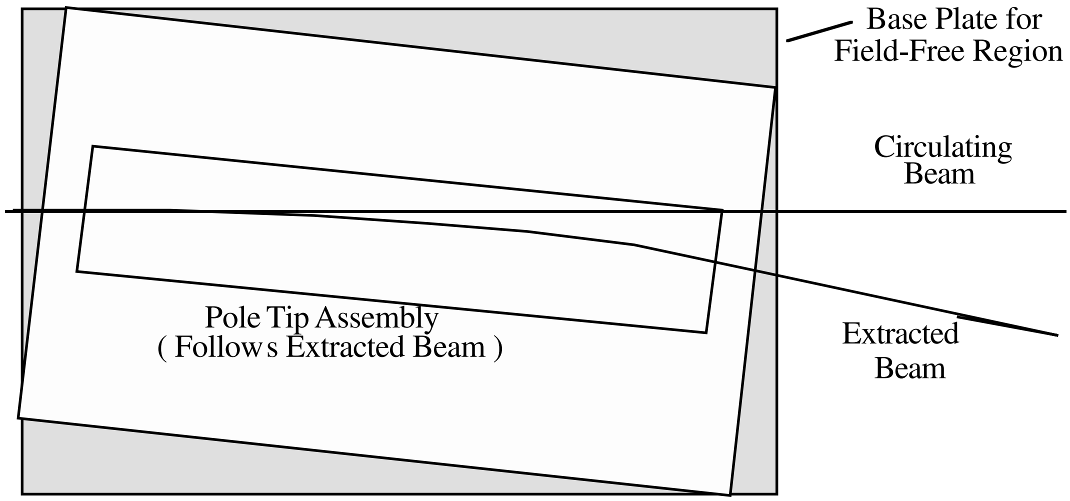


Figure 3.1.14: Side view of a Lambertson magnet showing the stored and extracted beam trajectories, and the slant in the extraction channel to minimize sagitta effects.

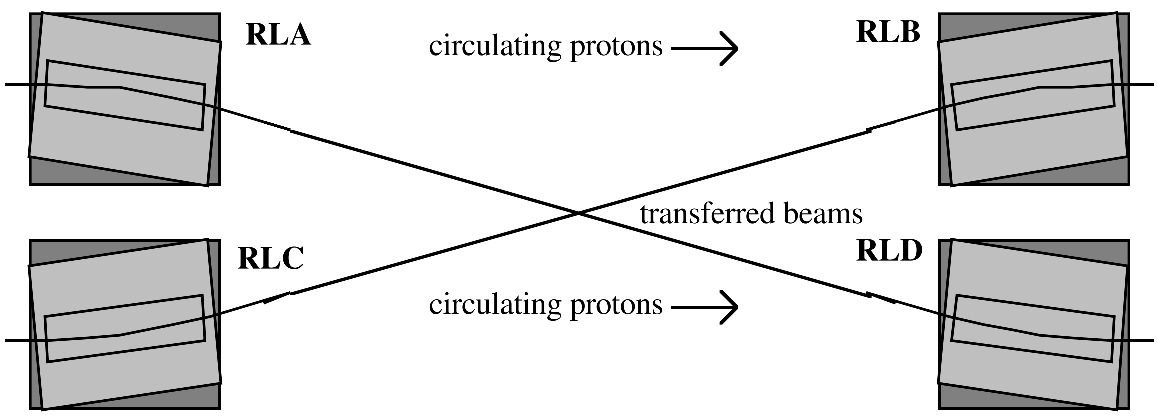


Figure 3.1.15: Lambertson construction geometries required to service all of the beam transfer needs of the Recycler.

To minimize sagitta and economize on magnet aperture, the pole tip assembly for the bend region follows (to first order) the trajectory of the deflected beam. The pole tip is therefore not parallel to the field-free trajectory, but is offset and canted by 1/2 of the bend angle or approximately 10 mrad. See fig. below. This is easily accomplished since the cutout of the field free region is machined out of the solid plates used to piece together the "base plate" of the Lambertson. See figure 3.1.14 for a sketch of the Lambertson geometry.

Two polarities of permanent-magnet Lambertsons are required: one which deflects counterclockwise protons (and clockwise antiprotons) downwards, and one which deflects them upwards. For each polarity there are two possible orientations of the "base plate" containing the field-free cutout: one which deflects incoming beam from the left, and another from the right. Figure 3.1.15 summarizes these options.

Two successful prototype permanent Lambertsons (2.2 kG and 3.55 kG, each 1m long) have been produced and tested. The bend field uniformity was adequate and the average field in the "field-free" region was <0.5 Gauss. The cross-sectional view of the permanent Lambertson is shown in figure 3.1.16.

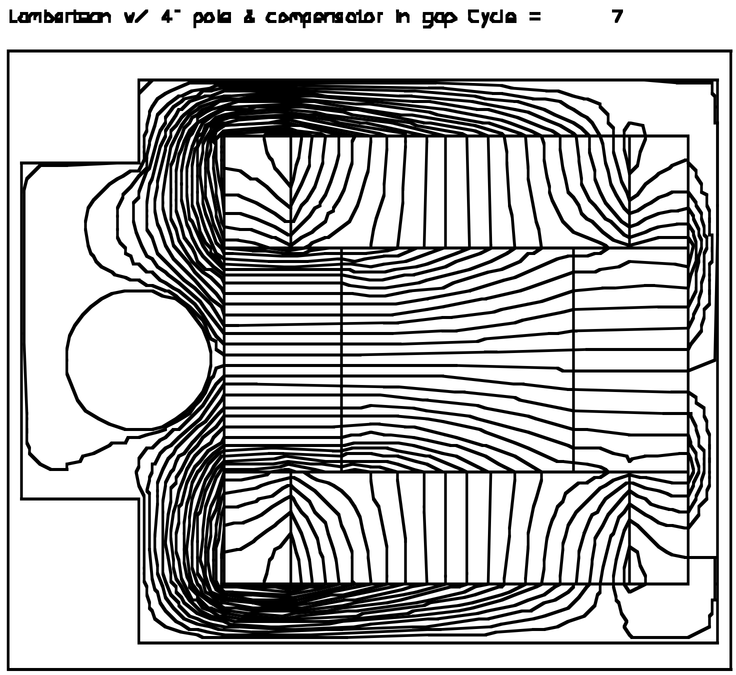


Figure 3.1.16: Permanent Lambertson magnet cross-section with POISSON field map superimposed. The field free circular region is the circulating beam aperture. The horizontal field in the extracted beam line steers the beam up or down. Three bricks drive flux into the central solid pole piece, one from the back and one from each side (top and bottom in the figure).

### *3.1.16: Magnet Hangers and Installation*

The hangers and installation for the Recycler are presently being modeled within the permanent magnet 8 GeV line project. It is expected that the magnets will be cheaper and easier to install than their Main Injector counterparts. For instance, each gradient dipole weighs approximately 1 ton, as compared to 20 tons in the Main Injector. The cross-section of the magnets are much smaller, and the magnets are shorter. The quadrupoles are expected to weigh approximately 200 lbs. each.

In most locations around the ring it is expected that the hangers will be bolted to the unistrut sections welded to the iron bars captured in the concrete tunnel walls. In a few locations where the tunnel shape changes or where Main Injector transfer lines to the Booster, Accumulator, and Tevatron exist, it will be necessary to build some more elaborate hangers.

## 3.2. Vacuum (WBS 3.1.2)

There are 104 cells in the Recycler ring. Because of the low outgassing rates accessible with the hydrogen degassing technique described in chapter 2, a vacuum pressure two orders of magnitude lower than the Main Injector can be achieved with the same number of pumps. In this discussion the type, placement, and processing of Recycler ring vacuum components are reviewed.

### *3.2.1. Geometry Overview*

In the Main Injector there are 6 ion pumps per cell and the length of vacuum sectors is approximately 500' (150 m). In the Recycler there will be one ion pump per cell, for a total of 104 ion pumps. Between the ion pumps there will be 5 titanium sublimation pumps (TSPs) per cell to achieve an average of pressure of approximately $1 \times 10^{-10}$ Torr. The benefit of TSPs are lower cost and lower ultimate pressures. Since the length of normal cells is 34 m and the length of dispersion cells is 26 m, the longest vacuum sector possible if the isolation valves are spaced every 8 cells apart is 270 m. Therefore, the total number of sector valves is $104 \div 8 = 26$. Figures 3.2.1 through 3.2.3 contain sketches of the vacuum system in normal arc cells, straight section cells, and dispersion suppression arc cells.

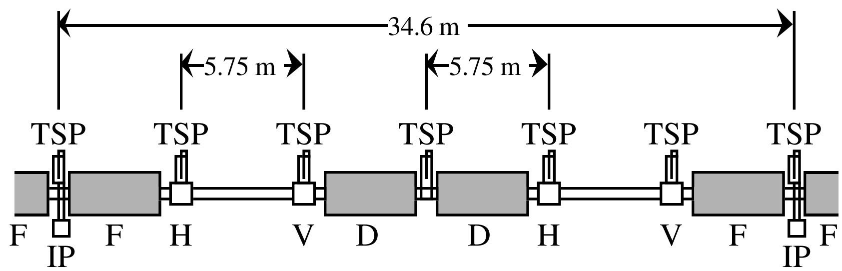


Figure 3.2.1: Sketch of the vacuum system in a normal arc cell. The horizontal (H) and vertical (V) beam position monitors have attached to them titanium sublimation pumps (TSP) in order to maintain a low average pressure and to minimize the number of welds in the tunnel.

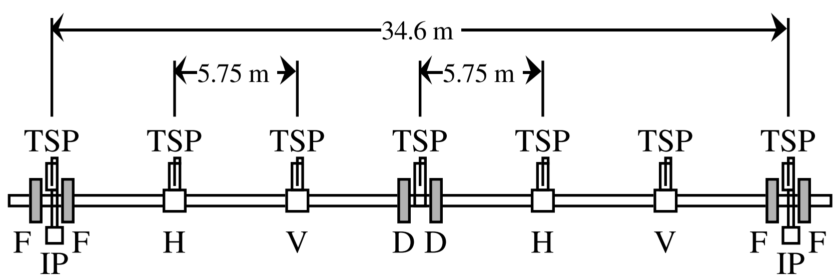


Figure 3.2.2: Sketch of the vacuum system in a normal straight section cell. Except for the fact that the quadrupoles are much shorter than the gradient magnets in the normal arc cell, nothing is different with respect to figure 3.2.1.

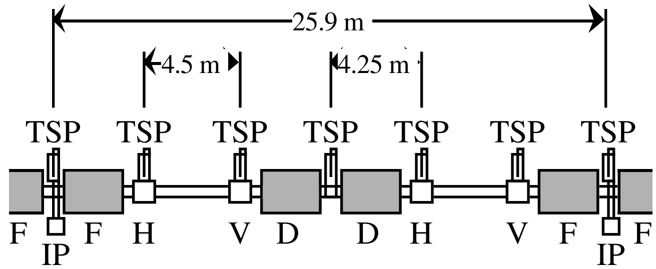


Figure 3.2.3: Sketch of the vacuum system in a dispersion suppresser cell.

With the exception of the MI-60 phase trombone straight cells which need additional vertical aperture and hence a round 3" O.D. beam tube, the Recycler vacuum tube is a 1.75" inside height by 3.75" inside width ellipse. It is produced by crushing a standard 3" O.D. beam tube with a wall thickness of 0.065".

### *3.2.2. Beam Position Monitor Assemblies*

In order to minimize the cost of the vacuum system, it is necessary to minimize the number of welds in the tunnel. This means generating as many pre-fabricated assemblies in industry and staging areas as possible. In addition, if possible it is good to merge multiple functionalities into the same component. For instance, the beam position monitor (BPM) can also act as an ion clearing electrode. Another possibility which will depend on further surface physics research by personnel at FNAL, LBNL, and KEK is the use of titanium electrodes in order to get ion pumping from the BPM electrodes.

Because both protons and antiprotons are injected into the Recycler for operations, commissioning, and studies, the beam position monitors need to be bi-directional. Capacitive split-tube electrodes are optimum in a geometry where the transverse beam size is comparable to the electrode dimensions. Capacitive electrodes are also perfect for the creation of ion clearing electrodes. In order to minimize the impedance effects of the BPMs, the electrodes are shaped to match the vacuum chamber, the outer wall of the BPM is the same shape as the electrodes and only large enough to stand off the 700 V of ion clearing voltage. For the same reasons, the gaps between the electrodes and the vacuum chamber wall are as small as possible without compromising the capacitance (and hence sensitivity) of the electrodes.

As can bee seen in figures 3.2.1 through 3.2.3, in every Recycler half cell there are always two BPMs separated by a straight, unoccupied section of vacuum pipe. At each of these BPM locations a bellow is required to absorb the length increase which occurs in the vacuum system when it is insitu baked at 150°C. In order to simply the beam pipe positioning stands and installation, the bellows are always located to the outside of both BPMs. As shown in figure 3.2.4, between the BPMs and bellows are TSPs. The TSP port is a rectangular slot 4" long and 1" high centered on the horizontal edge of the chamber (see figure 3.2.5). The horizontal edge of the vacuum chamber supports the minimum of the image current distribution, so therefore this geometry has the lowest impedance impact while simultaneously maximizing the conductance to the pump itself.

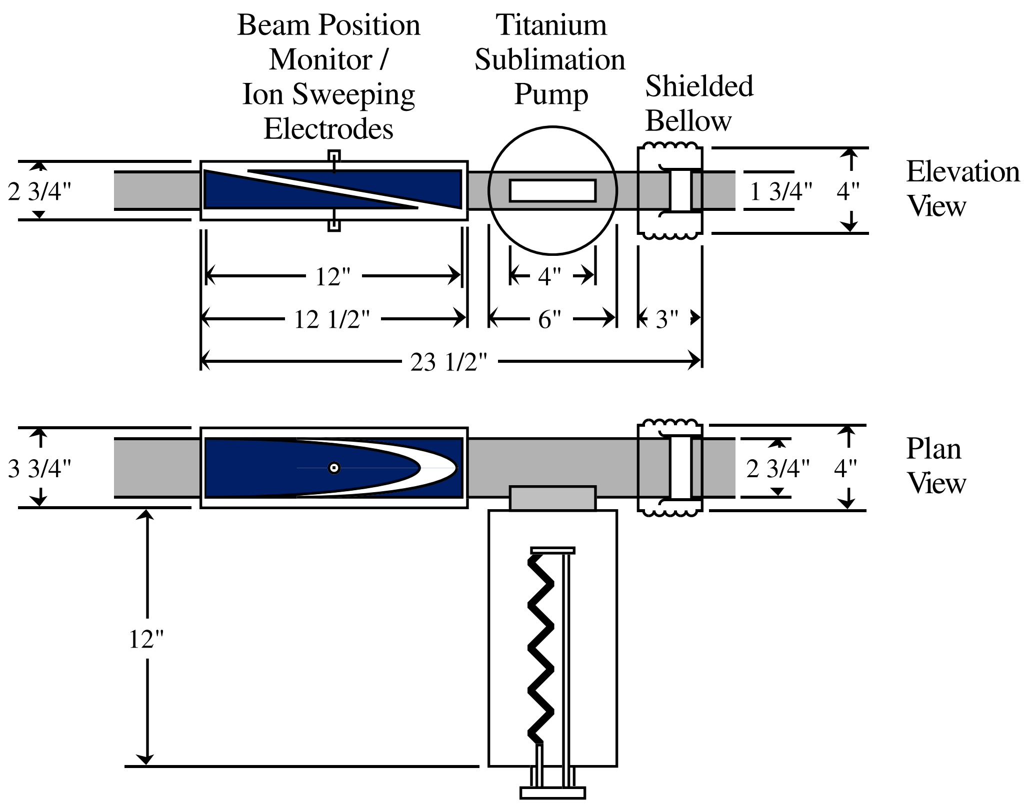


Figure 3.2.4: Elevation and plan views of the BPM assemblies which each include a TSP and shielded bellows. A vertical BPM is shown, which is on the downstream side of each half cell. The horizontal BPM, which is placed on the upstream side of each half cell, has a horizontally sensitive electrode and the entire assembly is rotated left for right.

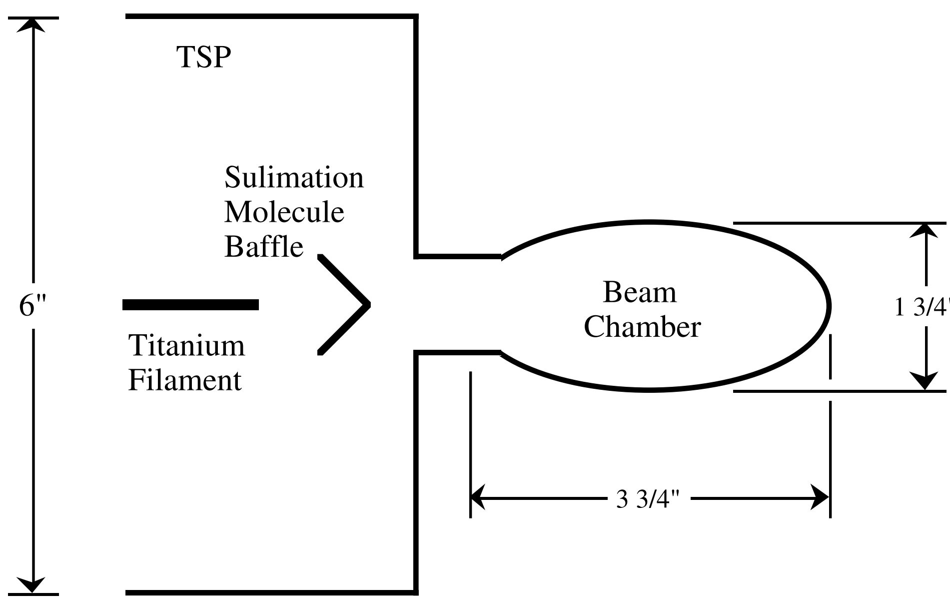


Figure 3.2.5: Beam's eye cross-section view of the TSP and its connection to the beam tube.

*3.2.3: Hydrogen Degassing Oven*

Before the hydrogen degassing is performed, the tubing is washed and cleaned internally with solvents. The tubing is then sent over to a former superconducting coil collar hydraulic press used for crushing the pipe into the correct elliptical shape. The design profile has an inner full height of 1.75 in. and a full width of 3.75 in.

In order to achieve this vacuum system configuration and achieve an average vacuum of approximately $1\times10^{-10}$ Torr, it is necessary to hydrogen degas every component. The test oven shown in figure 3.2.6 will be used for specialty pieces such as 1.5" diameter tubing for gauges. The 3" diameter tubing used to generate the vacuum chamber itself needs to be processed at a rate of approximately one half cell per day in order to keep up with the projected rate of magnet production. This criterion requires three 20' pipes per day. As shown in figure 3.2.7, by creating a new oven which has a 12" diameter, a total of six pipes per day could be processed. Since the processing requires that the tubing stay at a temperature of 500°C for approximately 12 hours (or 900°C for 30 minutes for those who prefer the higher temperature approach) and the time constant of the heating and cooling is approximately 4 hours, one batch of six pipes per day is a convenient processing rate. This requires that a technician spend approximately 1 hour per day to empty the previous day's tubing, clean the oven, load the next batch, and then start the control system computer which automatically performs the processing.

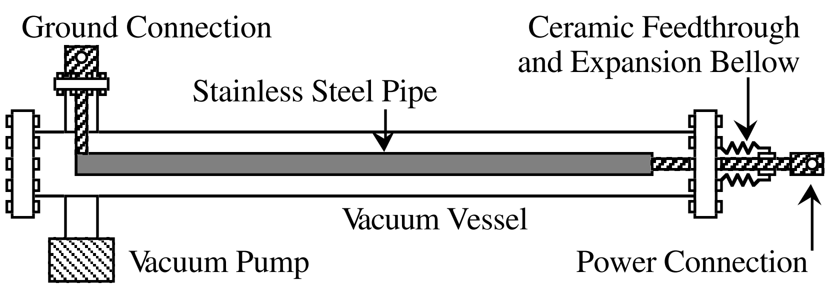


Figure 3.2.6: Sketch of the test oven which will still be used to process specialty tubing.

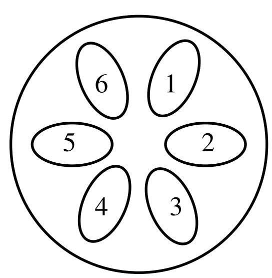


Figure 3.2.7: Profile of the crushed 3" tubing in the 12" diameter production oven proposed to generate an average of 2 half cells of tubing per day.

It is also necessary to hydrogen degas the tubing which makes up the beam position monitors, the titanium sublimation pumps, and also the shielded bellows. The split-plate capacitive pickups are created with the same 3" diameter tubing that makes up the rest of the vacuum system, unless the titanium electrode option is utilized. The 4.5" diameter tubing which forms the vacuum wall around the pickup electrodes, the 6" diameter tubing for the titanium sublimation pumps, and the bellows themselves are all hydrogen degassed before assembly. After the monitor, pump, and bellow has been assembled they are again baked to 500°C in order to burn off any surface hydrocarbons from the forming and assembly of the monitor, while simultaneously hydrogen degassing all of the miscellaneous steel parts such as end plates.

### *3.2.4. Shielded Bellows*

As shown in figure 3.2.4, associated with each BPM there is a bellow assembly. The bellows are shielded in a manner identical to the Main Injector. The reason for so many bellows is the 150°C bakeout which is necessary for initial vacuum commissioning. The coefficient of elongation of stainless steel tubing is 16 μm/m-°C. A normal half cell is 17 m long. Therefore, the 120°C temperature rise associated with the in-situ bake leads to a change in length of the beam tube of 33 mm or 1.25". Given that bakes are not expected to occur very often, a compression ratio of 2:1 is acceptable. Therefore, each half cell needs at least 2.5" of uncompressed bellow. Therefore, 2" of bellow at the horizontal BPM and 2" of bellow at the vertical BPM generate more than enough temperature change capacity. The other purpose of the bellows is to absorb approximately 0.5° of bend per bellow, since the pipe segments are straight.

### *3.2.5. Insitu Bake System*

After installation of the vacuum system it is necessary to heat it to 150°C for approximately 24 hours in order to purge the system of water vapor. But the entire 3.3 km circumference of the Recycler cannot be baked simultaneously. Instead, each vacuum sector is baked independently. As stated earlier, each vacuum sector is composed of 8 cells, or 16 half-cells.

The vacuum system is heated with the use of a pair of coaxial heaters. The coaxial geometry is used because of measurements performed on the 1 m long Recycler prototype gradient magnet where a DC 50 Amp current caused a $16 \times 10^{-4}$ field relative field deviation across the magnet aperture. By using a coaxial geometry, it can be assured that no field change will occur due to leakage fields from the heater conductors.

The thermal insulation around the vacuum chamber is integrated with the magnetic shielding around the chamber. As part of this system, there are 2 layers of insulation. In addition, the shining surface finish of the magnetic shielding also reflects back some heat.

In order for this scenario to work, a couple of conditions must be observed. First, the magnetic shielding around the beam pipe discussed in the next section must be electrically insulated from the beam pipe. Second, in order to evenly heat the vacuum chamber it is necessary to put in flexible copper ground straps across bellows to act as current bypasses. Thermal conduction through the stainless steel tubing is sufficient to heat the bellows.

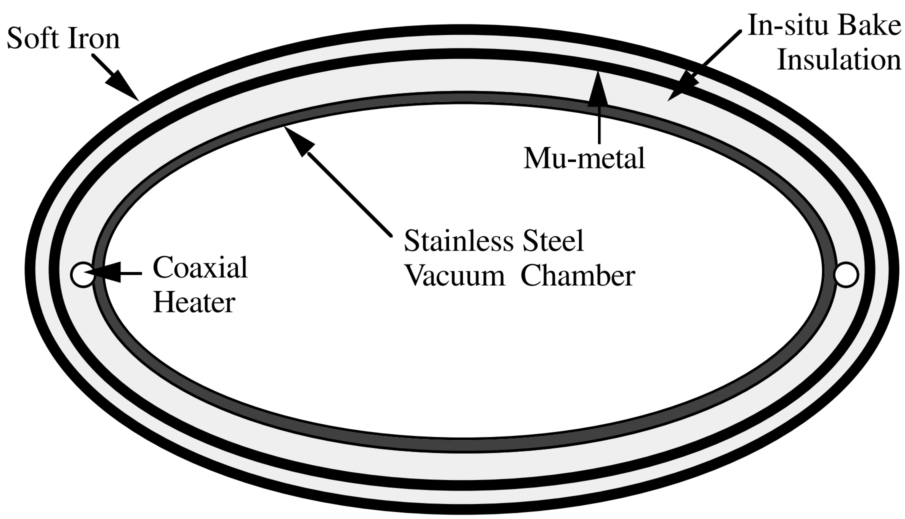


Figure 3.2.8: Sketch of the portable power supply connected across a vacuum sector used to heat the vacuum system to 150°C.

### *3.2.6. Magnetic Shielding*

Figure 3.2.8 contains a sketch of the magnetic shielding around the beam pipe at the edge of a permanent magnet. In order to prevent the Recycler beam from reacting to the Main Injector ramp, a hermetic magnetic seal around the Recycler vacuum chamber is required. In order to achieve a magnetic field reduction factor of 1000x, a layer of 4 mil thick mu-metal inside a 6 mil thick layer of soft iron is employed.

Between the vacuum chamber and mu-metal, and between the mu-metal and soft iron, are layers of thermal insulation. Not only is this insulation needed for the insitu bake system, but it is necessary to keep the mu-metal and soft iron from coming into contact in order to get the full magnetic field attenuation effect.

### *3.2.7. Beam Pipe Hangers*

It is necessary to build hangers specifically for the vacuum system due to the long distances between the magnets. The magnets themselves act as vacuum chamber hangers. In the center of the long sections between magnets the vacuum chamber hanger holds the pipe in a fixed position. During bakes the vacuum chamber lengthens toward the bellows near the beam position monitors. The hangers connected to these monitors have sliding joints which allow this expansion. Similarly, the pipe can slide within the magnets, but is held fixed at the end of the magnets at the 1 m short straights between the magnets. Figure 3.2.8 contains a sketch of this geometry.

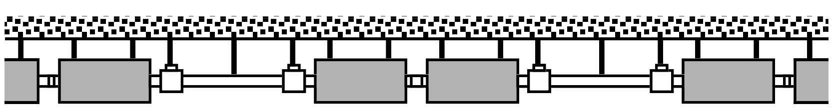

Figure 3.2.8: Magnet and vacuum chamber hangers for a normal cell. Note that the magnets themselves also act as vacuum chamber stands.

## 3.3. Power Supplies (WBS 3.1.3)

A total of 48 dipole correctors are needed in the Recycler ring and its dedicated transfer lines. The power supplies for these dipole correctors are only for limited orbit control around each of the 3 Lambertsons at MI-30 and MI-40 and their associated transfer lines. In addition, correctors are also needed at the kicker at MI-20. In order to generate an arbitrary position and angle in each plane, 8 dipole channels are required at each Lambertson in the Recycler. In addition, 4 horizontal and 4 vertical dipoles each separated by 90° of phase advance are necessary at each transfer line to adjust the position and angle into/out of the line. See figure 3.3.1 for a sketch of the locations of these correctors. At 6 Amps per channel and using the Main Ring corrector magnets, a deflection of 0.5 mr is achievable. Applied near a beta function maximum of approximately 50 m, a closed orbit motion of 25 mm is possible. Vertically this exceeds the 7/8" half height of the elliptical vacuum tube. The half width of the beam tube is just under 1-7/8", so only half the horizontal aperture can be probed by the beam center.

These power supplies are already existing Main Ring "ramped corrector" controllers which are not going to be used in the Main Injector. The correction magnets will also come from the Main Ring.

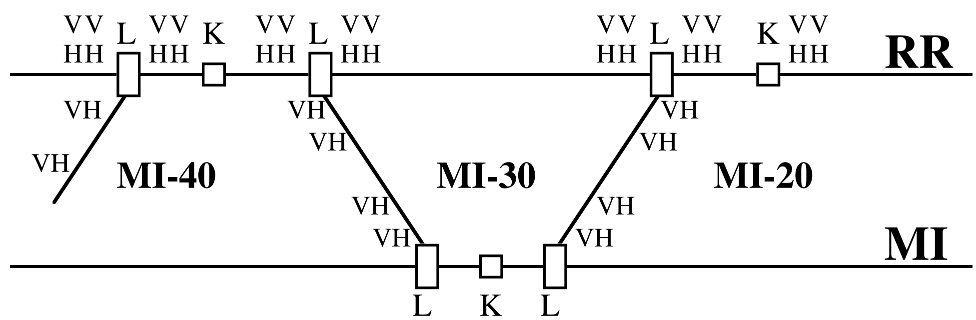


Figure 3.3.1: Locations of the horizontal (H) and vertical (V) dipole correctors in relationship with the kickers (K) and Lambertsons (L) required for the Recycler ring.

The ramped corrector power supplies are also used for three other powered magnet applications. The most important in the MI-60 phase trombone. Between each of the quadrupole pairs at MI-60 (and between the end quadrupoles and their partnered dispersion suppresser gradient magnets) a Main Ring correction quadrupole is installed. These 9 quadrupoles have enough strength to implement a phase trombone with a tuning range of greater than ±0.1 tune units.

Also at MI-60 two skew quadrupoles from the Main Ring will be transfered to the Recycler in order to implement global decoupling tuning. Because there are 6 corrector channels per chasis and the phase trombone only uses nine, the two skew quadrupoles will be plugged into the spare chassis channels.

Finally, 24 Main Ring sextupoles will be installed in the Recycler and powered individually with ramped corrector channels. At MI-20 and MI-50 two chassis each will be installed. In each pair of chassis 8 channels are dedicated to defocusing sextupoles and 4 are dedicated to focusing sextupoles. In all of the above applications the 6 Amp output of the ramped corrector power supplies is sufficient.

## 3.4. RF Systems (WBS 3.1.4)

The Recycler RF system is both very simple and highly complex. Because the Recycler ring is fixed energy, coordinated control of voltage, synchronous phase, radial position, tuning angle, cavity resonant frequency, grid bias, etc. is not necessary. On the other hand, the barrier bucket manipulations outlined in chapter 2 represent a quantum leap in phase agility and computer control.

### *3.4.1. High Level System*

The RF cavities for the Recycler acceleration system are actually 50Ω ceramic gaps which have sufficient inductance to pass frequencies above 10 kHz. Four of these cavities are used to generate the needed peak voltage of 2 kV.

Connected to each of these cavities is a 5 kW amplifier and a gap monitor signal which feeds back into the feedback system which insures fidelity to the programmed waveform and suppression of beam loading voltages. The amplifiers have a highpass cutoff frequency of 10 kHz and a lowpass cutoff frequency of 100 MHz. All of the amplifier feedback electronics and control electronics are in the MI-60 service building.

### *3.4.2. Low Level System*

Most of the hardware, firmware, and software necessary for the Recycler RF system is already being generated for the Main Injector RF system. Therefore, the estimation of manpower and hardware do not represent as large a level of extrapolation as might be expected.

The system revolves around a very advanced direct digital synthesizer VME module which allows computer coordinated frequency changes which are phase continuous. By programming frequency ramps, arbitrary relative phases can be generated between neighboring synthesizers. Since all synthesizers run off of the same clock, frequency synchronization is a digital control with no phase lock loops or feedback systems necessary. By sending this 52.8 MHz sinusoid through a comparator and a divide by 588 counter, a turn marker can be generated which is extremely phase agile. By sending that pulse into a module which under computer control generates a pulse of arbitrary length and height, the full capability of the RF system described in chapter 2 is realized.

The Direct Digital Synthesizer (DDS) VXI LLRF platform component offers performance improvement and new implementation options for transfer synchronization. The DDS includes an AD21062 SHARC DSP, Harris Numerically Controlled Oscillators (NCO), and RF parts for SSB modulation. The DDS has three RF outputs; $RF_1=A\sin(\omega t+\Phi_1)$ , $RF_2=A\sin(\omega t+\Phi_2)$ , and $RF_3=A\sin(\omega t+\Phi_3)$. Under DSP control, the outputs are frequency and phase agile, with controlled $\Phi_n$ and its first through third derivatives. The $\omega t$ term is determined from a 720 Hz MDAT input, filtered, and updated at 100 kHz identically for all RF outputs. The DSP updates $\Phi_n$ with 16.66 kHz and 100 kHz components that include absolute and relative phase terms. $\Phi_n$ registers also sum a $\Delta\Phi_n$ term for phase control at precise rates. This specifies cogging processes directly in the fundamental unit of interest, instead of the present cogging system's $\Delta\Phi_{cog} = \int\Delta\Phi\ dt$, taken over the cogging interval.

For the Recycler, two DDS modules are employed in parallel to generate six independent phase-variable waveforms which can be used to generate and manipulate barrier buckets. Figure 3.4.1 contains a block diagram of this system. All six waveforms are created by sending the DDS channel sine waves into comparators which generate pulses at 52.8 MHz. The divide-by-588 circuit generates a single pulse each turn, which in itself triggers an arbitrary waveform generator. All six waveforms are then summed before being delivered to the high level RF system.

Unlike the Main Injector, the Recycler store beams for long periods of time. Therefore, an added constraint for Recycler operations is that the phase and amplitude noise of the pulses be very small. Measurements of the spectral purity of the output of the comparator are very promising.

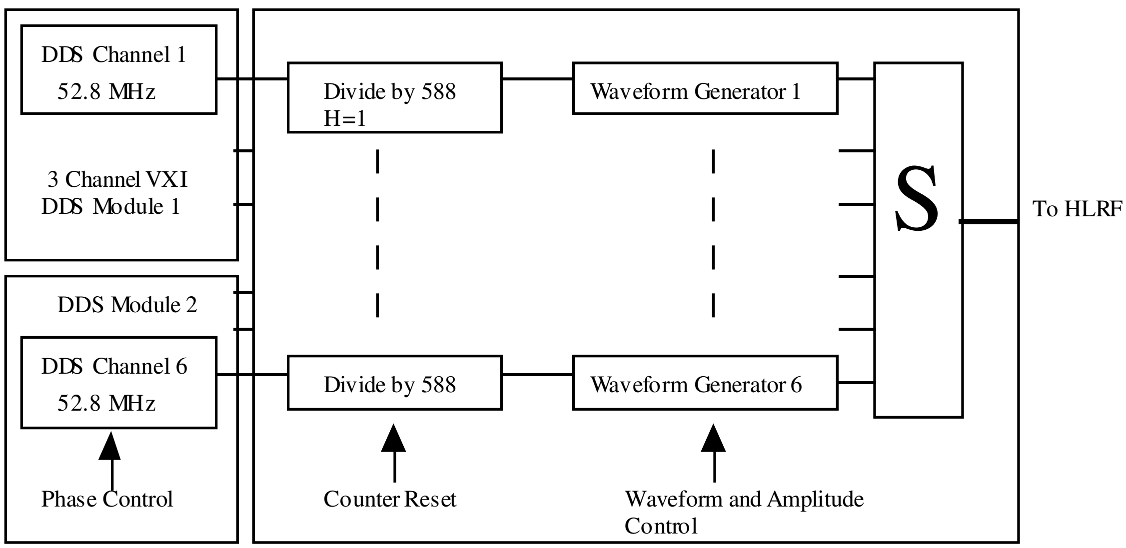


Figure 3.4.1: Block diagram of the Recycler low-level RF system.

## 3.6. Kickers (WBS 3.1.6)

The specifications for the kicker magnets needed for Recycler operations are listed in table 3.6.1. In order to keep costs low, the kicker in the Recycler ring should build on the Main Injector design experience as much as possible.

Table 3.6.1: Specifications for the Recycler magnet kickers and the transfer kicker in the Main Injector for injection/extraction with respect to the Recycler.

| Location | Direction | Kick | Risetime | Falltime | Flattop | Recharge |
|---|---|---|---|---|---|---|
| RR-20 | Horz | 300 G-m | 1-2 µs | 1-2 µs | 1.6 µs | 10 sec |
| MI-30 | Horz | 300 G-m | 1-2 ns | 1-2 µs | 1.6 µs | 10 sec |
| RR-40 | Horz | 300 G-m | 1-2 µs | 1-2 µs | 1.6 µs | 10 sec |

A design which comfortably attains the specifications has been produced. Parts from old Main Ring systems and the production of systems similar enough to the Main Injector to share spare capacity have been designed. No unusual technology was invoked to reach the above parameters.

## 3.7. Stochastic Cooling (WBS 3.1.7)

There are 4 stochastic cooling systems envisioned for the Recycler ring. The two transverse systems are 2-4 GHz bandwidth betatron cooling systems. Providing momentum cooling are a pair of systems; a 1-2 GHz and 0.5-1 GHz filter cooling system.

### *3.7.1. Pickup and Kicker Placement*

As shown in figure 3.7.1, an amplitude modulated laser beam is used to cut a chord across a potion of the ring to transmit the signals from the pickups to the kickers. The laser beams should propagate down evacuated tubes in order to prevent excessive laser attenuation during periods of poor weather. Another benefit of laser propagation through an evacuated tube is the insensitivity of time-of-flight to humidity and air pressure changes.

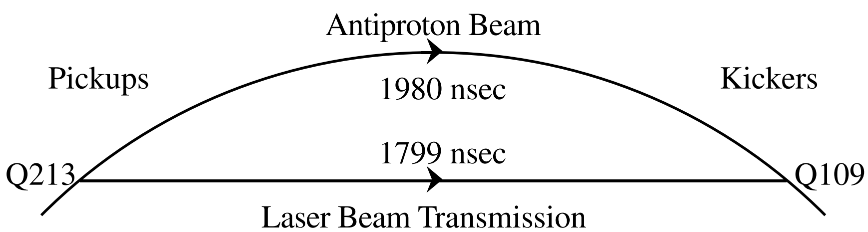


Figure 3.7.1: The chord cut by the stochastic cooling systems in order to minimize the bad mixing between the pickup and kicker.

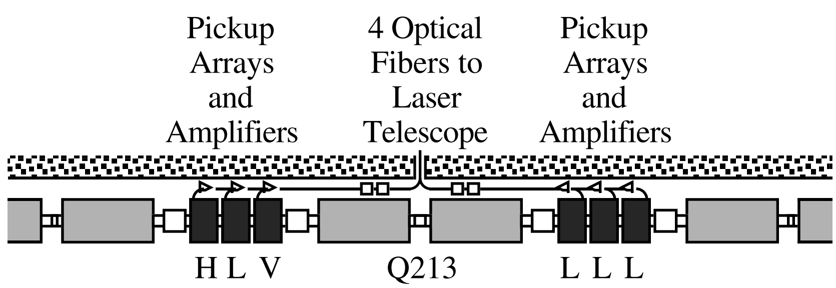


Figure 3.7.2: The relative placement of the horizontal (H), vertical (V), and momentum (L) pickup tanks with respect to the magnets. Note that the pre-amplifiers are attached to the tanks, while the laser driver for the optical fiber signal transmission are placed over the permanent magnets in order to obtain some radiation shielding from Main Injector losses.

The placement of the pickup tanks around Q213 is shown in figure 3.7.2. The pre-amplifiers are attached to the pickup tanks, while the power amplifiers and optical fiber transmitters are placed over the permanent gradient magnets for radiation shielding against Main Injector losses. At Q109 the relative tank placements are identical, and the fiber optic receiver and power amplifiers are again over permanent gradient magnets. The final power amplifiers, planned to be travelling wave tubes (TWTs), are attached to the kicker tanks themselves.

### *3.7.2. Arrays and Tanks*

The number of pickup and kicker tanks and pickup and kicker electrodes are listed in table 3.7.1. As the frequency of the system increases, the size of the electrodes and their spacing along the beam shrink. Therefore, the higher frequency systems have a higher longitudinal density of electrodes.

Table 3.7.1: Number of pickup and kicker tanks and electrodes required to fulfill the cooling requirements outlined in chapter 2.

| Plane | Band (GHz) | Pickup Tanks | Kicker Tanks | Pickup Electrodes | Kicker Electrodes |
|---|---|---|---|---|---|
| Horz | 2-4 | 1 | 1 | 32 | 32 |
| Vert | 2-4 | 1 | 1 | 32 | 32 |
| Mom | 1-2 | 2 | 2 | 32 | 32 |
| Mom | 0.5-1 | 2 | 2 | 16 | 16 |
| | Total | 6 | 6 | | |

The standard length of a tank is 48". A typical array is 1 m long. Therefore, only three tanks per half cell fit into an unmodified section of Recycler lattice.

### *3.7.3. Laser Telescope*

The laser telescope is composed of two passive elements per beam, each pair on either side of the telescope. First, in order to minimize the laser beam divergence the beam radius is increased via large aperture telescope lens systems at either end of the evacuated tubes. With a 20:1 expansion ratio, the laser beam can be as large as 2" in diameter. Second, the transitions of the laser light from fiber optic cable to air and back are accomplished with a light launcher composed of a polished fiber end coupled to a point-to-parallel collimating lens.

As shown in figure 3.7.3, there are also X-Y micro-positioning stages to move the light launcher transversely with respect to the beam expander and to steer the entire beam in either dimension. These stages are operated via remote control and/or feedback loops to set and maintain a high quality optical link across the arc of the Recycler.

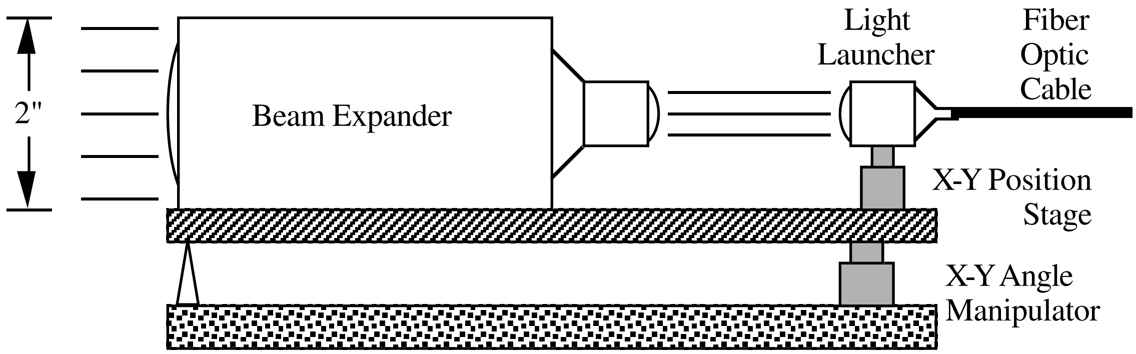


Figure 3.7.3: Sketch of the optics involved in the laser telescope. The passive optical hardware is identical on both sides of the telescope.

## 3.8. Instrumentation (WBS 3.1.8)

The Recycler Ring instrumentation will closely resemble much of the Main Injector instrumentation. The beamline intensity monitors and both the longitudinal and transverse wideband detectors will be identical. Some changes will occur in the transverse Schottky system to take advantage of the stationary revolution frequency of the Recycler. A commercial beam current measurement system will be purchased. Due to costs and unusual beam signals, the beam position monitor system is very unique.

### *3.8.1. Beam Position Monitor System*

The BPM (Beam Position Monitor) detectors will be used for both position information and ion clearing. In the Recycler ring 416 detectors located at the 1/3 and 2/3 boundaries of each half cell will provide 8 detectors per betatron wavelength in both the horizontal and vertical planes. Split-plate detectors will provide output linear with displacement in one plane at a time. Three flavors of detector will be required: one horizontal and one vertical elliptical detector, covering most of the ring; and one round detector, rotated to measure the desired plane. Detector edges will be rounded to prevent arcing of the ion-clearing high voltage.

The BPM system will have two measurement modes. The first measures injected beam from the Booster or Main Injector, while the second measures the closed orbit of the stack. The beam stack in the Recycler will be DC beam, except for an injection gap equal to 1/7th of the circumference. For both modes, the resulting harmonics of the 89.8 kHz revolution frequency lead to an AC-coupled pulse for low frequency processing.

The low and medium frequency response of the detector resembles that of a highpass filter. The low frequency corner is inversely proportional to both the terminating resistance and the system capacitance. For long cable runs terminated in high impedance, sensitivity is inversely proportional to the cable capacitance. These two factors dictate the use of high-impedance pre-amplifier buffers in the tunnel. A series resistance before the pre-amp reduces the system bandwidth and noise. The radiation resistance of possible pre-amp candidates is being tested in the Booster dump. Manufacturer testing [Analog Devices, Inc., Radtest Data Service, November 1995] claims radiation resistances of 25-

50 and 200 kRad for two possible chips. Other possibilities, including discrete transistors, are being considered.

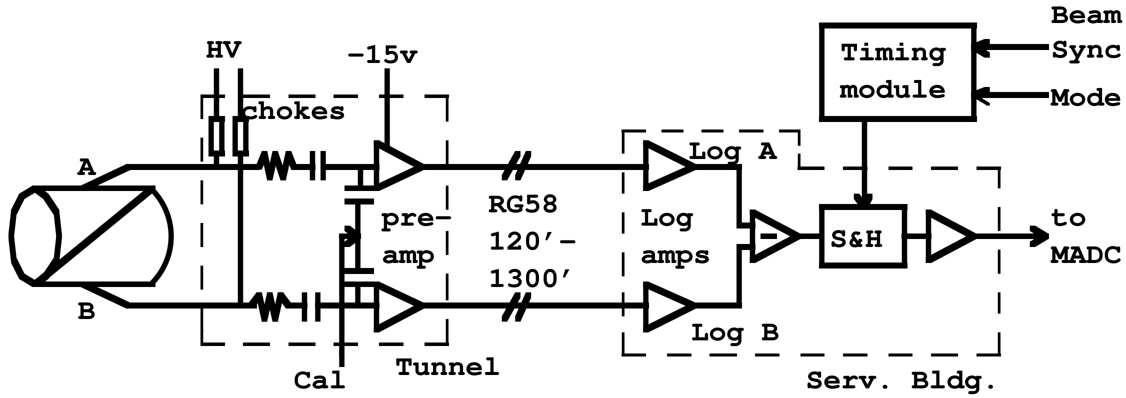


Figure 3.8.1: Block Diagram of the Recycler BPM System.

Short cables will connect detector feedthroughs to a small shielding box for the pre-amps and other components. The box, shared by two neighboring detectors, may be mounted above the Recycler magnets for enhanced radiation shielding. A high resistance couples the high DC voltages to the detector plates for ion clearing. The high voltages are daisy-chained for all the detectors in a sector. Current monitoring takes place at the source of these voltages, in the service buildings. A calibration signal, resembling a typical signal pulse, will also be daisy-chained throughout a sector. When activated, it will be loosely coupled equally to the two signal paths.

The low signal frequencies enable use of inexpensive RG58 50Ω cable for the 120'-1300' cable runs. Additional cables are needed for the two pre-amp DC supplies, the ion-clearing high voltage, and the calibration signal. Dual use of cables for DC and AC signals is being considered. Figure 3.8.1 contains a sketch of the BPM system.

The cost constraints of the Recycler project and the nature of the detector signals demand a new, inexpensive processing scheme and control system interface. Innovations in analog processing technology and the Fermilab control system make that possible.

The position can be derived from the signals of a linear detector by

$$\frac{x[\mathrm{mm}]}{b[\mathrm{mm}]} = \left(\frac{A-B}{A+B}\right) \approx \frac{\mathrm{Ln}10}{2}\left(\log A - \log B\right) \quad , \qquad (3.8.1)$$

where A and B are amplitudes of the two plate signals and b is the detector radius. Recent improvements in logarithmic amplifiers [Analog Devices, Inc., AD640 and AD608 data sheets, Analog Devices Design-In Reference Manual, 1994] enable a large dynamic range and high bandwidth. Laboratory tests on a simulated Recycler signal show a dynamic range near 50 dB. These chips approximate the log function. Log nonconformance, which leads to errors, is expected to fall within the accuracy specification. Subtraction by a differential op-amp results in a voltage which is converted to position after system (detector and electronics) offset subtraction and scaling. This can be carried out in the control system.

The position signal will be digitized using standard MADC-compatible ADCs from the Controls Department. The result is interfaced to the control system with the CAMAC 290 MADCs. The differing signal occurrence times at the BPMs (a range of 2 μs per sector for both protons and antiprotons) and the two operating modes (injection and stack) require a sample-and-hold circuit with correct timing. From the 1.6 μs minimum signal length, acquisition time, and other factors, it is anticipated that 6 distinct timing signals are needed per house. These will be created with CAMAC 279 modules, synchronized to the Recycler Ring Beam Sync clock.

The digitized signals are converted into ACNET database devices with scaling as described above. Standard acquisition types will be available, including "snapshot" (closed-orbit), "flash" (single-turn), and turn-by-turn (TBT). Note that only one TBT channel is possible per MADC, and current plans call for two MADCs per house. An application page will control acquisition modes and timings, as well as calibrations done during beam-off times.

### *3.8.2. Beam Loss Monitor System*

The Recycler Ring will use the beam loss monitor system of its neighbor, the Main Injector. There will be no additional monitoring for the Recycler.

### *3.8.3. Longitudinal Wideband Pickup*

One resistive wall current longitudinal pickup will be built for the Recycler and placed in the MI-30 region. The design will be identical to that used for the Main Injector. It will be used for studies and any possible longitudinal monitoring systems.

The basic design of this resistive wall current monitor is to insert a ceramic gap shunted with resistance in the vacuum pipe and measure the voltage induced by the beam wall current [R. Webber, "Longitudinal Emittance an Introduction to the Concept and Survey of Measurement Techniques Including Designing of a Wall Current Monitor", AIP Acc. Instr. Conf. Proc. #212, 1989]. The ultimate bandwidth of such a detector is limited by the spreading of the electric field lines between the beam and the image charge on the inside wall. For the monitor's 5" circular aperture and the relativistic Recycler beam, the bandwidth limit is 23 GHz.

In practice the detector response is difficult to maintain above the microwave cutoff frequency of the beam pipe, estimated to be 1.4 GHz for the 5" diameter. Spurious electromagnetic energy, generated by various discontinuities and guided along the beam pipe, corrupts the image current signal. Microwave absorber material is placed inside a 6" vacuum pipe up and downstream of the detector to reduce this noise by 20 dB. The absorbing material is an epoxy-based Resin Systems RS4825 core. It is placed outside a 5" aperture ceramic sleeve to preserve vacuum specifications without lessening the absorbing properties. This solution is cheaper and more readily available than the previous vacuum-friendly absorber.

The detector maintains a 3 kHz low frequency cutoff with a series of toroids shunting the resistance across the gap. An impedance of 1Ω (122 resistors of 112Ω each) terminates a radial transmission line formed by the 140 mil ceramic gap. Four signal pickoff points spaced evenly around the gap are summed to reduce position dependence and azimuthal signals. The result is a position-independent longitudinal monitor with ±1 dB flat response from 3 kHz to 6 GHz, as measured with a tapered 50Ω transmission line test setup. An identical, reciprocal port can be used for calibration.

### *3.8.4. Transverse Wideband Pickups*

The Main Injector transverse wideband pickup design will be used in the Recycler. Two pickups, one for each plane, will be placed at MI-30 for studies purposes.

Standard striplines are planned for both the horizontal and vertical planes. Feedthroughs at both ends will be used to observe both proton and antiproton signals. The plate length of 55", $\lambda/4$ at 53 MHz, will be used to increase signal and to maximize doublet separation when viewing proton injections. In the frequency domain, zeroes in transmission will occur at those frequencies where the plate is $\lambda/2$ long.

### *3.8.5. Transverse Profile Monitors*

The Ionization Profile Monitor (IPM) system [Zagel, J., "Fermilab Booster Ion Profile Monitor System Using LabView", AIP Acc. Instr. Conf. Proc. #333, 1994], used in the Booster and Main Ring/Main Injector, is planned for the Recycler Ring. Two systems are needed to handle the transverse planes. The IPM uses a microchannel plate to collect and amplify ions produced when the beam passes through residual gas in the detector. The high quality vacuum in the Recycler may necessitate an intentional, localized, calibrated gas leak at the IPM detector.

The 8 kV clearing field of the Booster IPM sweeps the ions across the 10 cm aperture onto a microchannel plate, which amplifies the current and deposits it onto a grid of 1.5 mm spaced conductors etched into a printed circuit card. The current induced in each conductor is amplified, digitized, and stored each turn. The amplifiers have a gain of 2.5 X $10^6$ volts per amp and 100 kHz bandwidth. The digitizers are commercial 4 channel 12 bit VME cards which have 64 Kwords of memory for each channel. A National Instruments MXI adapter is used to access the VME cards with a Macintosh computer running LabView software. The Main Ring IPMs use a 20 kV clearing field across the 10 cm aperture with 0.5 mm conductor spacing on the collection grid.

A flying wire system is not being included due to the high reliability demanded of the Recycler ring. The possibility of the failure mode of the wire getting stuck in beam was considered too great.

### *3.8.6. Transverse Schottky Monitor*

The Recycler Ring transverse Schottky monitor system [Chou, P., "Transverse Schottky Detector for Antiproton Recycle Ring", internal Fermilab note] will be similar to the new Main Ring system but with much higher sensitivity. The primary system output is a two channel (for two planes) spectrum analyzer display in the main control room. Various beam parameters can be calculated from information provided by transverse Schottky signals, including fractional tune, transverse emittance, momentum spread, chromaticity, and presence of trapped ions [Peterson, D., "Schottky Signal Monitoring at Fermilab", AIP Acc. Instr. Conf. Proc. #229, 1990].

The two Schottky detectors, to be located at MI-30, will be round, split-plate capacitive pickups. A box in the tunnel will contain a transformer, designed to resonate the detector at 79.263 MHz and to couple to the output cable. The resonant frequency was chosen at the harmonic number n=882.5, halfway between the first two harmonics of the Main Injector RF system. A bandwidth of 90 kHz (one revolution harmonic) requires a loaded quality factor $Q_L$=880. To enable this high Q and maintain stability, suitable feedthroughs must be found and temperature drift effects must be small. The detector sensitivity is given by

$$S_{\perp} = \frac{l}{2bc}\sqrt{\frac{R_o\,\omega_c\,Q_o}{C_t}} \quad , \qquad (3.8.2)$$

where l is length, nominally 40 cm, b is aperture radius, c is speed of light, $R_o$ is the receiver's 50Ω termination, $\omega_c$ is radian resonant frequency, $Q_o$ is unloaded Q, and $C_t$ is total capacitance. Design calculations estimate a sensitivity of 22 Ω/mm, much higher than the Main Ring system (0.9 Ω/mm) and comparable to the Tevatron's (27 Ω/mm). Low-loss heliax 50Ω cables will be used to bring the signals upstairs.

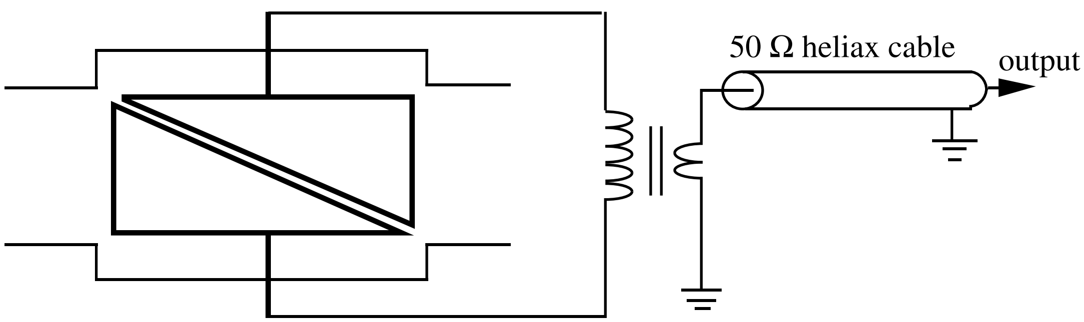


Figure 3.8.2: Sketch of the Recycler transverse Schottky electrical model. The split plate pickup provides a linear position response function. The system is resonated at 79.263 MHz (n=882.5).

The Schottky receiver down-converts the signal bandwidth to baseband for use with a low frequency spectrum analyzer. A Trontech ultra-low noise amplifier provides 60 dB of gain. Variable attenuators tune the gain. Custom crystal bandpass filters from Piezo Technology, Inc. set the signal bandwidth at 100 kHz. The local oscillator signal might be generated by a Main Injector injection frequency oscillator, if available, or a fixed custom oscillator. Unlike the Main Ring/Main Injector, the Recycler energy is constant at 8.9 GeV. Thus, its revolution harmonics will remain fixed and no frequency tracking is needed. A mixer down-converts the signal before a final low-pass filter and gain stage. A long length of RG-8 low loss cable brings the outputs to the Main Control Room and the spectrum analyzer. Given that a horizontal and vertical system are needed, this implies 2 cables to the control room and two channels of FFT capable digitizers.

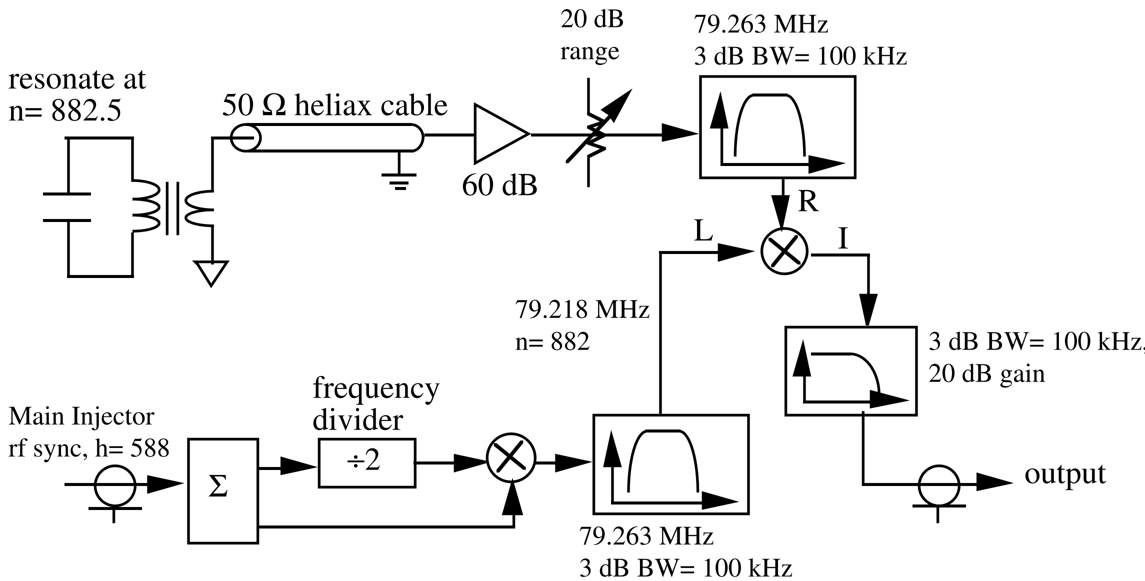


Figure 3.8.3: Sketch of the beam processing electronics which conditions the RF signal from the detector to a low frequency signal a signal analyzer can measure.

### *3.8.7. Ring Current Monitor (DCCT)*

The DC Current Transformer, or parametric current transformer, uses the second harmonic detection principle to measure the DC beam current in series with an AC transformer to extend the bandwidth (Unser, K., "The Parametric Current Transformer, a beam current monitor developed for LEP", AIP Acc. Instr. Conf. Proc. #252, 1991). Fermilab does have a number of versions of the DCCT, but a commercial version will be purchased for a Recycler unit at MI-30. The Bergoz current monitor (Bergoz, Parametric Current Transformer data sheet) is 4.25" long and offers several apertures from 2" to 7". At this time, a 3" pipe is anticipated at MI-30. A ceramic break is required for use with the Bergoz monitor. Radiation damage can be reduced by selecting the radiation hard sensor option and locating the tunnel front-end electronics (maximally 5 m from the sensor) where radiation dosage is less than $10^4$ rad/year.

The DC current monitor is relied upon for absolute beam current calibrations. The Bergoz monitor specifies a frequency response from DC-20 (optionally 100) kHz, dynamic range of 2 X $10^7$ for each full scale range, resolution optionally to 0.5 µA, and absolute accuracy and linearity of 0.05% and 0.01%, respectively. The ±10V output is digitized and interfaced to the controls system with the MADC.

### *3.8.9. Toroids*

Toroid systems are AC-coupled intensity monitors that are cheaper than DCCTs and appropriate during transient events such as injections and extractions. The present toroid design used Pearson Electronics, Inc. model number 3100 current monitors. The aperture is 3.5" and the output signal is 0.5 volts/amp into 50Ω with a bandwidth of 40 Hz to 7 MHz. At the toroid output the signal is 85 mV for $10^{10}$ ppb. The toroid is electrically isolated from ground in the enclosure and good quality cable such as LDF4-50A is required to avoid noise problems. The toroid must be placed over a ceramic break in the vacuum pipe. To reduce the RF energy radiated into the environment a ground connection is required across the break but external to the toroid.

The signal is transported to the service building where the electronics amplifies, limits the bandwidth, and integrates the signal to provide a voltage representing the total charge. The present design [Vogel, G., "Toroid Integrator User Guide", internal Fermilab note] in use includes a baseline subtraction circuit, a fixed length integration window, and an A/D and D/A used to form a sample and infinite hold. The toroid integrator has a bandwidth of 100 Hz to 400 kHz and selectable gains of $2\times10^{11}$, $2\times10^{10}$, and $2\times10^{9}$ particles/volt.

There are 6 toroid systems required due to the addition of the Recycler Ring. Figure 3.8.4 shows the relative locations of these systems. For each transfer between the Main Injector and the Recycler there are 3 toroids; one to determine the initial intensity, one record the transfer line intensity, and finally one to measure the final intensity. For the abort line there is an initial intensity and an abort line intensity.

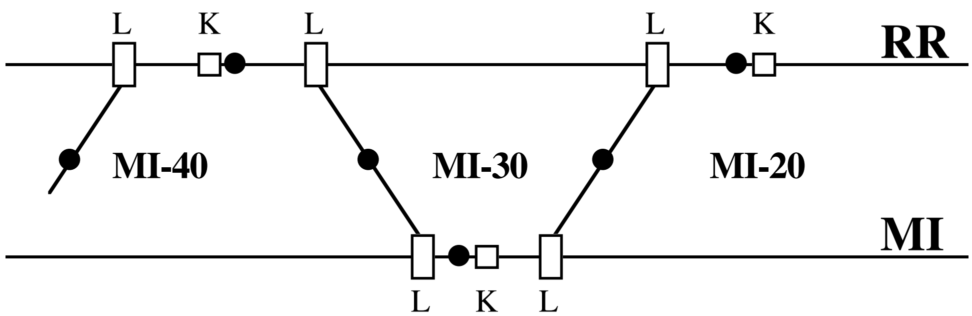


Figure 3.8.4: Sketch of the placement and number of toroids in the Main Injector and Recycler to service the instrumentation needs of the Recycler transfers. The Lambertsons (L), kickers (K), and toroids (black dots) are shown with respect to the service building the reside in.

## 3.9. Controls (WBS 3.1.9)

Controls requirements have been the focus of a number of cross-departmental discussions. Because of the novel nature of many of the technologies employed in the Recycler ring, it is important that a thorough exploration of hidden demands on controls be identified. Just as in the case of beam instrumentation, it is vital for efficient commissioning of the Recycler that all control software and hardware be installed and tested before actual accelerator commissioning commences. Below is the result of these scope explorations.

### *3.9.1. Stochastic Cooling System*

Existing equipment will be moved from the present Tevatron bunched beam stochastic cooling R&D implementation. CAMAC equipment now residing at F0 TeV crates $60, $61, $62 will be moved to their new locations at MI-20 and MI-30.

### *3.9.2. Power Supplies*

The two kickers in the Recycler and one kicker in the Main Injector will need power supply controllers - CAMAC C118 cards and beam synch triggers supplied by C279 cards. All associated Lambertsons are built with permanent magnets and do not require power supply controls.

There are a number of dipole correctors required in the Recycler ring and its transfer lines. Around each of the 3 Recycler Lambertsons a 4-bump orbit offset is required in both planes. This requirement alone involves 24 correctors. In the transfer and abort lines another 20 correctors are required. Figure 3.3.1 contains a sketch of the corrector count and placement.

In addition to the dipole correctors, the phase trombone quadrupoles, the two skew quadrupoles at MI-60, and the correction sextupoles at MI-20 and MI-50 are also powered with Main Ring ramped corrector chasis.

All correctors will utilize existing MR corrector power supplies and existing corrector coils, each chassis controls 6 correction elements. A total of 8 of these supplies are required: 2 at MI-20, 4 at MI-30, and 2 at MI-40. It should be noted that additional bulk power supply control in addition to what CAMAC 053 cards can provide is required. Six CAMAC 118 cards will be included to cover this need.

### *3.9.3. RF Systems*

The low level RF system developed for the Recycler RF system, which is a copy of the VXI MI LLRF system, will be located at MI-60. It will need an accelerator controls ethernet connection to the VXI platform.

### *3.9.4. GPIB Interfaces*

Stochastic cooling, RF, and instrumentation all need GPIB connections. There will be an interface at MI-20, MI-30, and MI-60 (assuming up to 32 devices per connection). A high speed and reliable VME based interface will be used.

### *3.9.5. Vacuum System*

There will be one ion pump for every 2 half cells (104 total) for the Recycler itself. There will also be 4 pumps for each of the transfer lines (16 total). Each pump requires control and monitoring. No automatic valves (other than the safety critical devices) will be allowed in the Recycler in order to eliminate the chance of accidental antiproton stack loss. All of the valves will be manually operated. The positions of these manual valves will not be electronically monitored. Instead, valve motion will only be allowed via the insertion of keys which can only be removed when the valves are in the out position. The keys are put in a low-tech key tree to make up a permit. The requirement for gauges is two ion gauges per vacuum sector (every 8 cells for a total of 13 sectors and 26 gauges). CIA crates are the best way to effect control of Recycler pumps. Spare control channels are available in planned Main Injector CIA crates at 4 of the 6 service buildings. Two CIA crates (and ARCNET controllers) will be purchased for the other service buildings. One CIA card can control 6 pumps. Some spare gauge channels will be used by the Recycler. Sharing CIA crate space with the Main Injector vacuum system will not present any software problems. Summary of ring and transfer line (XL) pumps and their geographical position are summarized in table 3.9.1.

Table 3.9.1: Summary of the Recycler pump controller locations around the ring. Transfer line (XL) pumps are also included in the count.

| Service Bldg | # of Cells | Ring Pumps | XL Pumps | Total Pumps |
|---|---|---|---|---|
| MI-10 | 16 | 16 | 0 | 16 |
| MI-20 | 16 | 16 | 0 | 16 |
| MI-30 | 20 | 20 | 8 | 28 |
| MI-40 | 16 | 16 | 2 | 18 |
| MI-50 | 16 | 16 | 0 | 16 |
| MI-60 | 20 | 20 | 0 | 20 |
| Totals | 104 | 104 | 10 | 114 |

### *3.9.6. Beam Position Monitors (BPM)*

It is possible to support the Recycler BPM system with existing multiplexed ADC (MADC) and CAMAC 290 card controllers dedicated to this function. Scans of the closed orbit can occur every 1 to 2 seconds. Turn-by-turn beam position acquisition is also supported. For turn-by-turn data taking, the MADCs (and controllers) must be fast enough to accommodate the Recycler's 90 kHz revolution frequency. A minimum 12 bit resolution for the MADC has been specified.

There is one horizontal and one vertical BPM every half cell, for a total of 416 Recycler ring beam position measurements. Intensity signals will not be provided by the BPM RF modules. Horizontal and vertical monitors are distributed to separate MADCs to facilitate acquiring turn-by-turn data. This will require at least two MADC systems per house (service building). Connection to the sample and hold analog outputs of the BPMs should be direct and use 16 twisted pair cable for direct connection to the MADC. Avoiding use of an Analog Entry Box will save costs.

Table 3.9.2: Summary of BPM MADC system counts and locations.

| Service Bldg | # Cells | Horz BPMs | Vert BPMs | XL BPMs | Total BPMs |
|---|---|---|---|---|---|
| MI-10 | 16 | 32 | 32 | 0 | 64 |
| MI-20 | 16 | 32 | 32 | 0 | 64 |
| MI-30 | 20 | 40 | 40 | 28 | 108 |
| MI-40 | 16 | 32 | 32 | 8 | 72 |
| MI-50 | 16 | 32 | 32 | 0 | 64 |
| MI-60 | 20 | 40 | 40 | 0 | 80 |
| Totals | 104 | 208 | 208 | 36 | 452 |

Associated control of BPM data acquisition requires generation of a "sample" signal triggered by a RRBS event. Also required at each service building are four CAMAC

279 cards listening for the sample event to provide appropriately timed triggers to the BPM module's sample-and-hold (S&H) circuit. The data taking mode of the CAMAC 290 cards is controlled by TCLK events and software. A timing resolution of 1 µsec is required for BPM signal sampling.

There are also BPMs associated with each of the transfer lines. These are included in table 3.9.2 as "XL BPM", with half being horizontal and the other half vertical. The ring beam sync timing will also serve to trigger the S&H circuits of the transfer line BPMs.

#### *3.9.7. Control System Front Ends*

Recycler controls requirements do not require an additional front end computer. Specialized instrumentation systems such as residual gas ionization profile monitors using Macintosh computers running the LabView software are connected directly to the ethernet link around the ring.

#### *3.9.8. Accelerator Control Consoles*

An MI-30 control room for Recycler commissioning and electron cooling research, development, and eventual commissioning will need two consoles.

#### *3.9.9. Beam Permit System:*

Because of the precious nature of antiprotons, the beam permit system will only be applied to protons during commissioning. The Recycler beam permit system status will be applied to the beam switch sum box (BSSB) to adjudicate injection of protons. CAMAC 200 cards, input panels, and repeaters will be installed at each of the 6 Main Injector service buildings and the main control room. All equipment should be available from the MR system after decommissioning. The beam permit will be physically implemented with a spare optical fiber.

#### *3.9.10. Recycler Ring Beam Sync Clock (RRBS)*

The low level RF system will provide: a revolution marker (53 MHz/588); 7.5 MHz (53 MHz/7), and 53 MHz. Various CAMAC modules are necessary for clock generation and have been added to the WBS. These will be located at MI-60 and include two CAMAC 377 cards, a CAMAC 280, 175, and 276 card. These signals will be supported ring-wide and at the main control room, so at least 12 fiber repeaters are necessary. RRBS will use a spare optical fiber.

#### *3.9.11. Software*

Unlike the Main Injector, in which most systems existed previously in the Main Ring, the Recycler relies on new subsystems, new geometries, and hence new software. Because of the traditional tendency to underestimate software manpower requirements, serious discussions of the scope of software requirements have been held. Below are the results of these discussions.

*Database entries:* The stochastic cooling system gets transferred from the Tevatron. Everything else is created new. Because of the use of permanent magnets, the nonexistence of distributed corrector systems, and the lack of utilities, the total number of database entries is <1000. A new "R" index page will be created and R:xxxxxx database entries will be facilitated.

*Applications:* After studying the applications driving the other Fermilab accelerators, a list of programs relevant to the Recycler ring has been developed. Some of the applications are rather generic, such as DataLogger, vacuum readback, and parameter pages. The orbit control/magnet move program is very important, and is already applied to Fermilab accelerators. With the addition of the Recycler lattice to the program database, it will be able to function with minimal modification. Similarly, the stochastic cooling software already exists from the Tevatron Collider bunched beam cooling effort. New programs for low level RF control and beam position measurement must be written. Just as the number of database entries is orders of magnitude smaller than other accelerators, the number of application programs is similarly low.

## 3.10. Safety System (WBS 3.1.10)

The additional safety system components necessary to support the Recycler are quite limited. To insure the termination of the coasting beam in the Recycler, two gravity activated fail safe vacuum isolation gate valves will be used. These valves are necessary because permanent magnets cannot be readily turned off and interlocked.

## 3.11. Utilities (WBS 3.1.11)

Besides a limited amount of conventional power, the only utility being used by the Recycler is LCW. The subsystems which consume this water are described below. All usages are in service buildings. Note that the total water flow required by the Recycler is approximately 40 gallons/minute. There are sometimes leaks in the Main Ring that are larger than this!

### *3.11.1. Dipole Corrector Supplies*

The dipole correctors supplies at MI-10, MI-30, and MI-40 require 4 gallons/minute per chassis. Each chassis services 6 correctors. Table 3.11.1 summarizes this usage.

Table 3.11.1: Summary of LCW water usage rates at each service building in which a need exists for the ring and its dedicated transfer lines.

| Location | # Chassis | LCW Need |
|---|---|---|
| MI-20 | 4 | 6 gal/min |
| MI-30 | 4 | 16 gal/min |
| MI-40 | 2 | 8 gal/min |
| MI-50 | 2 | 8 gal/min |
| MI-60 | 2 | 8 gal/min |

### *3.11.2. Stochastic Cooling Traveling Wave Tubes*

The stochastic cooling kickers at MI-30 are driven by traveling wave tubes (TWT) which require a couple of gallons per minute per tube. Given that there are three cooling channels, a total of approximately 6 gal/minute is required.

### *3.11.3. Moving Existing LCW Pipes*

There are a limited amount of valves, pipes, and air dehumidifiers which have already been installed in the MI-60 straight section which will have to be moved because of the addition of the Recycler. In addition, in order to build the MI-22 and MI-32 transfer lines between the Main Injector and Recycler the LCW headers in the regions between Q212 & Q222 and Q320 & Q330 need to be moved.